

## Structure and electrical conduction properties of phthalocyanine thin films

R.D. Gould

*Thin Films Laboratory, Department of Physics, Keele University, Keele, Staffs ST5 5BG, UK*

Received 20 October 1995

### Contents

Abstract	237
1. Introduction	238
2. Structure	239
3. Dc electrical properties	246
3.1. Basic conduction processes	248
3.2. Space-charge-limited conductivity	254
3.3. The Poole–Frenkel effect	258
3.4. Variable range hopping conduction	259
3.5. Tunnelling	261
3.6. The Schottky effect	262
3.7. Diode-type conductivity	264
4. Ac electrical properties	266
5. Summary and conclusions	270
Acknowledgements	272
References	272

### Abstract

The structure and the dc and ac electrical conduction properties of evaporated phthalocyanine thin films are critically reviewed.

Results of various structural studies on phthalocyanine single crystals and thin films performed using X-ray diffraction methods are described, and reported unit cell dimensions are given for several phthalocyanines in both the metastable  $\alpha$  and the stable  $\beta$  forms; reported unit cell dimensions for both the monoclinic and triclinic forms of the atypical lead phthalocyanine, are given. Recent work on the  $\alpha$  to  $\beta$  phase transformations and growth in phthalocyanine films, the dependence of structure and preferential orientation on film thickness and substrate temperature, and observations of the monoclinic and triclinic phases in lead phthalocyanine films are also discussed.

The importance of the type of electrical contacts applied and the existence of surface states in sandwich structures of phthalocyanine films are stressed, and a summary of the various dc

conduction processes observed is given, together with the relevant theoretical conductivity equations. Selected results on samples showing ohmic and space-charge-limited conductivity, the Poole-Frenkel effect, variable-range hopping, tunnelling, the Schottky effect and diode-type conductivity are compared, the present state of knowledge is summarized and suggestions for further work are proposed. Ac measurements on phthalocyanine films using both blocking and ohmic contacts are described, together with an account of equivalent circuit models adopted to account for the dependences of capacitance and loss tangent on frequency and temperature. Several sets of measurements of ac conductivity as a function of frequency, which usually show a power-law dependence, are compared and associated with hopping conduction in the lower temperature range. Free-band conductivity at higher temperatures is also reviewed.

Finally, constraints placed on the making of electrical measurements by the necessary use of materials less pure than those of the inorganic materials customarily used in semiconductor technology and the tendency for phthalocyanine films to absorb oxygen is emphasized. The use of improved materials deposition and characterization in future work is recommended.

**Keywords:** Phthalocyanine; Thin films; Electrical conduction; Structure; Unit cell dimensions

---

## 1. Introduction

The early history of the synthesis and properties of the phthalocyanines has been fully described by Moser and Thomas [1]. Briefly, metal-free phthalocyanine ( $H_2Pc$ ) was first synthesized in 1907 by Braun and Tcherniac, and the metal-substituted copper phthalocyanine ( $CuPc$ ) was originally manufactured in 1927 by de Diesbach and von der Weid. Following this, many other metal-substituted phthalocyanines were synthesized and a comprehensive study of their chemical properties was initiated by Linstead and coworkers in 1934 [2]; Linstead also coined the term “phthalocyanine” to refer to this class of organic materials.

The structure of the planar phthalocyanine molecule was first reported by Dent et al. [3], and consists of four isoindole units linked by aza nitrogen atoms and surrounding two hydrogen atoms. In the simple metal phthalocyanines, such as  $CuPc$ , the two central hydrogen atoms are replaced by a single metal atom. A major property related to this structure is that generally the various phthalocyanine molecules are thermally stable and can thus be sublimed without decomposition. Therefore, in contrast with many other organic compounds, the preparation of phthalocyanine thin films by vacuum evaporation is feasible.

Semiconducting behaviour was originally observed in the bulk phthalocyanines in 1948 by Eley [4] and Vartanyan [5]. In due course these measurements were followed in 1963 by those of Heilmeyer and Warfield [6] on single crystals of  $H_2Pc$ , which showed space-charge-limited conductivity (SCLC), a conduction mechanism previously described by Rose [7]. In the same year Heilmeyer and Harrison [8] reported initial electrical measurements on  $CuPc$  single crystals, which were followed 4 years later by the classic paper of Sussman [9] which unequivocally identified SCLC in  $CuPc$  thin films; an accompanying paper [10] described the sensitivity of  $CuPc$  films to ambient gases such as nitrogen, hydrogen and oxygen, and effectively laid the foundations for much of the subsequent work on phthalocyanine gas detectors.

More recently, it has been established that phthalocyanine thin films do not only exhibit SCLC, as reported by Sussman [9] and Hamann [11], but may also display other high-field conduction processes such as the Schottky and Poole–Frenkel effects [12,13]. Furthermore, since the structure of lead phthalocyanine (PbPc) phases has been established for both the monoclinic [14] and triclinic [15] forms, thin films of this material have been proposed for gas sensing applications [16,17]. These developments have been instrumental in stimulating renewed interest in the electrical properties of a wide range of phthalocyanine thin films, and also in their structural features. In this short review some selected aspects of the structure and electrical properties of phthalocyanine thin films will be described with particular, but not exclusive, emphasis on work performed in the last decade. There will be no attempt to describe the purification, deposition or the particular gas sensing properties, the latter of which have been previously covered up to 1989 in the excellent review by Wright [18]. Similarly, the chemistry involved in the addition of side-groups to various phthalocyanine molecules in order to provide soluble materials for Langmuir–Blodgett deposition will not be covered. Instead the emphasis will be on the physics of phthalocyanine thin films and the various processes which give rise to electronic conductivity. The coverage is not intended to be exhaustive, but rather to illustrate some of the more interesting and exciting aspects of phthalocyanine thin films.

The review will commence with a short summary of the structural features of phthalocyanine thin films, usually obtained by X-ray diffraction. These features are discussed primarily from the point of view of their dependences on the substrate temperature during deposition and of the film thickness. The importance of the film structure to the electrical properties has been evident since the work of Wihksne and Newkirk [19] on pressed pellets of the metastable  $\alpha$  and the stable  $\beta$  forms of  $H_2Pc$ , which revealed that the electrical conductivity of the  $\alpha$  phase was considerably greater than that of the  $\beta$  phase, by a factor of nearly  $10^5$ . This will be followed by a discussion of the dc electrical properties of phthalocyanine thin films, with particular emphasis on the high-field electrical conduction processes observed. Ac properties, mainly the dependence of conductivity, loss tangent and capacitance on frequency and temperature, will also be briefly covered.

## 2. Structure

X-ray diffraction studies were originally made by Robertson [20] on the metal-free, nickel, copper and platinum compounds. These measurements were performed on crystals of the  $\beta$ -form material. Robertson pointed out that the crystal structure of  $H_2Pc$  and many of the metallic derivatives, including  $CuPc$ , are dimensionally very similar. The structure is monoclinic with two molecules per unit cell. The quoted unit cell dimensions and interplanar angles were as follows:  $a = 1.985$  nm,  $b = 0.472$  nm,  $c = 1.48$  nm and  $\beta = 122.25^\circ$  for  $H_2Pc$ ;  $a = 1.96$  nm,  $b = 0.479$  nm,  $c = 1.46$  nm and  $\beta = 120.6^\circ$  for  $CuPc$ . Ebert and Gottlieb [21] studied polymorphism in the phthalocyanines, and published X-ray diffraction traces for the  $\alpha$  and  $\beta$  forms of  $CuPc$ ,  $H_2Pc$  and the cobalt, nickel and zinc phthalocyanines ( $CoPc$ ,  $NiPc$  and  $ZnPc$  respectively). The most significant feature of these traces was the two intense

but distinguishable peaks for the  $\beta$  form in all the materials investigated, while for the  $\alpha$  form this was replaced by a single intense peak at a similar angle. Shortly after the appearance of this work, Karasek and Decius [22] performed more detailed X-ray diffraction measurements on  $H_2Pc$  for both polymorphic forms. The  $\alpha$  form was produced by sublimation onto a rock salt plate maintained at a temperature below  $200^\circ\text{C}$ . Although the first peak in the  $\alpha$ -form pattern was of significantly lower intensity than that observed previously [21], this was related to preferential orientation effects provided by the substrate. The growth of  $\alpha$ -form, rather than  $\beta$ -form, sublimed films was attributed to the relatively low substrate temperature, which was below the  $\alpha$  to  $\beta$  phase transition temperature. Robinson and Klein [23] made detailed X-ray diffraction measurements of  $\alpha$  CuPc and measured the intensities and interplanar spacings for 29 different diffraction lines. These values were consistent with a tetragonal structure with unit cell dimensions  $a = 1.7367\text{ nm}$  and  $c = 1.279\text{ nm}$ . However, this designation was questioned by Assour [24] who suggested that his own X-ray data on the  $\alpha$  polymorph of CuPc implied an orthorhombic rather than a tetragonal structure. Furthermore, he argued that in fact the previously proposed  $\gamma$  phase of CuPc was essentially the same as the  $\alpha$  phase, apparently differing only in the degree of resolution. Ashida et al. [25,26] made electron diffraction measurements on  $\alpha$ -form films deposited onto muscovite, and associated the data with a monoclinic structure for CuPc, CoPc,  $H_2Pc$  and NiPc, as well as iron and platinum phthalocyanines (FePc and PtPc respectively). The following unit cell dimensions were derived for the first two of these:  $a = 2.592\text{ nm}$ ,  $b = 0.379\text{ nm}$ ,  $c = 2.392\text{ nm}$  and  $\beta = 90.4^\circ$  for CuPc;  $a = 2.588\text{ nm}$ ,  $b = 0.375\text{ nm}$ ,  $c = 2.408\text{ nm}$  and  $\beta = 90.2^\circ$  for CoPc. The fact that the angle  $\beta$  is very close to  $90^\circ$  is consistent with the previous orthorhombic designation by Assour [24]. A schematic diagram of the molecular arrangement proposed for the  $\alpha$  and  $\beta$  forms of CuPc is shown in Fig. 1. The major difference between the two arrangements is in the tilting angle of the molecular plane

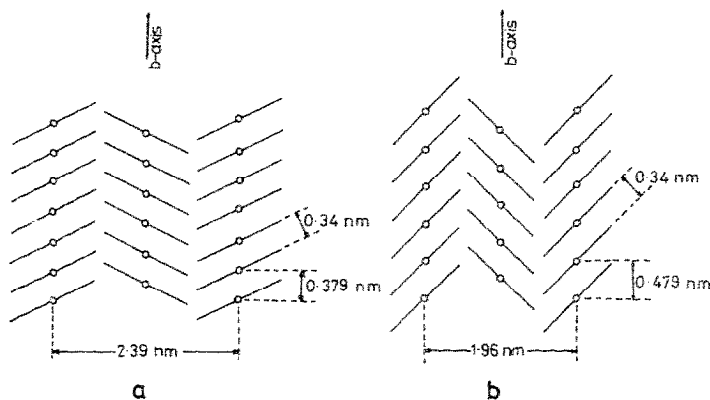


Fig. 1. Molecular arrangements in copper phthalocyanine crystals of (a) the  $\alpha$  form and (b) the  $\beta$  form. Adapted with permission from Ref. [26].

to the stacking axis. The molecular planes incline at an angle of  $26.5^\circ$  in the  $\alpha$  form [26] and  $46.8^\circ$  in the  $\beta$  form [27]. However, because  $\alpha$ -form single crystals of reasonable size cannot normally be prepared by sublimation, a comprehensive X-ray analysis of the type performed for the  $\beta$  phase by Robertson [20], and more recently confirmed by Brown [27], has not been performed. Perhaps the most comprehensive measurements on the  $\alpha$  polymorph are also those of Brown [28] on PtPc: in this work the calculated and observed structure amplitudes were reported for a considerable number of reflections. These measurements were performed on microscopic crystals with a cross-section of less than 0.01 mm, which were recovered from Linstead's laboratory. The structure was reported to be monoclinic with unit cell dimensions similar to those reported by Ashida et al. [25]. However, the angle  $\beta$  was reported to be  $94.3^\circ$ , somewhat exceeding the previous value of  $91.9^\circ$ . The impetus for this work was to determine the structure of the  $\alpha$  form of CuPc, using the well-known similarities between the structures of the two materials. Therefore some uncertainty remains concerning whether the  $\alpha$  phase is tetragonal, orthorhombic or monoclinic, although more recent work on NiPc and CoPc films has compared derived unit cell dimensions only with those of the proposed monoclinic structure [29]. Additionally, it has also been argued that even the  $\beta$ -form unit cell dimensions of PtPc originally derived by Robertson are incorrect, and that a different monoclinic unit cell exists [25]. Nevertheless, it is still relatively straightforward to distinguish between the  $\alpha$  and  $\beta$  phases on the basis of X-ray diffraction, and the phase identification can be confirmed using other techniques such as IR absorption spectroscopy [21,30] or, for the case of paramagnetic metallic derivatives, electron spin resonance studies [31].

More recently a substantial body of work has been performed on phase transitions from the  $\alpha$  to the  $\beta$  phase, and on aspects of the growth of various phthalocyanine films. Iwatsu et al. [32] studied ZnPc, in particular the  $\alpha$  to  $\beta$  phase transition.  $\alpha$ -form ZnPc was prepared by the acid paste method and the phase transformation was observed by monitoring X-ray diffraction behaviour during the course of exposure to various alcohol vapours. Measurements of microcrystallite size were obtained by the Debye-Scherrer method, which involved measurement of the width of the line profile of the (200) reflection and yielded a value of 14.7 nm. Mindorff and Brodie [33] observed phase changes in  $H_2$ Pc vacuum-deposited films. A smooth progression from an amorphous structure through the  $\alpha$  phase to the  $\beta$  phase was observed on annealing from room temperature to 515 K. By using scanning electron microscopy Boudjema et al. [34] found that the microcrystallite size in their  $\alpha$ -form films of NiPc and ZnPc were in the range 50–100 nm. Komiyama et al. [35] grew ultrathin CuPc films by molecular beam deposition, and their X-ray diffraction patterns exhibited an intense single diffraction peak at  $2\theta = 6.75^\circ$ , indicating a strong preferential orientation. Neutron diffraction measurements [36] on CoPc yielded refined values of the unit cell dimensions for the monoclinic  $\beta$  phase of  $a = 1.9352$  nm,  $b = 0.4773$  nm,  $c = 1.4542$  nm and  $\beta = 120.82^\circ$  at 295 K, while a comprehensive charge density structure was also derived by the same group [37]. Debe and Kam [38] carried out a remarkable series of experiments on CuPc films grown by closed-cell physical vapour transport in a microgravity environment in low Earth orbit on the

Space Shuttle Orbiter. Together with the preceding and following papers by members of the same group, this work covered the effects of gravity on the homogeneity and microstructure of the films, as well as reporting a new microgravity thin-film polymorph, designated M-CuPc. A very useful discussion of the various other CuPc polymorphs reported previously was also given [38].

Hassan and Gould [39] carried out a comprehensive structural investigation of CuPc thin films prepared by thermal evaporation, using X-ray diffraction and IR absorption methods. The evaporant powder was of the  $\beta$  form, and exhibited X-ray diffraction features similar to previously published data for  $\beta$ -form CuPc [24,30,38] and  $\beta$ -form  $H_2Pc$  [22]. Additional peaks in the diffraction patterns that were also observed by Assour [24] were identified with the existence of minor proportions of other CuPc polymorphs or remaining impurities. The material was evaporated onto glass substrates maintained at room temperature and therefore formed films of the  $\alpha$  phase. Fig. 2 shows X-ray diffraction traces for three different films deposited at the same rate of  $0.5 \text{ nm s}^{-1}$ , but with different thicknesses of  $0.1 \mu\text{m}$ ,  $0.8 \mu\text{m}$  and  $1.5 \mu\text{m}$ . The thinner film shows only a single peak, which is labelled as (001) using an indexing scheme based on the original structural determination of Robinson and Klein [23]. However, if the structure of  $\alpha$  CuPc is of the more recently proposed

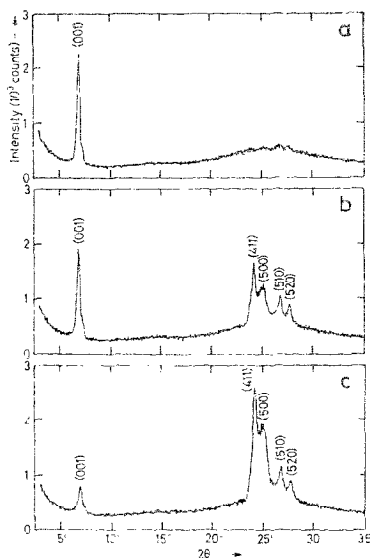


Fig. 2. X-ray diffraction traces obtained from primarily  $\alpha$ -form CuPc thin films with thicknesses of (a)  $0.1 \mu\text{m}$ , (b)  $0.8 \mu\text{m}$  and (c)  $1.5 \mu\text{m}$ . Intensity relates to a step size of  $0.02^\circ$  sampled for 1 s. The peaks are labelled according to the tetragonal scheme and are indexed differently if the structure is orthorhombic or monoclinic, as explained in the text. Reproduced with permission from Ref. [39].

orthorhombic or monoclinic structures [24,25,28], then the peak corresponds to the (200) reflection. The pattern is very similar to that described for films of thickness 38 nm [35], showing a comparable highly oriented morphology. As the film thickness increased, additional reflections were observed for  $22^\circ < 2\theta < 28^\circ$ . These peaks, indexed as (411), (500), (510) and (520), or as (11 $\bar{1}$ ), (11 $\bar{2}$ ), (11 $\bar{3}$ ) and (313) for the orthorhombic or monoclinic systems, have been identified with reflections from lattice planes within a stack along the *b* axis [38]. Therefore the phthalocyanine film structure departed from that of a strong preferential orientation in the [001] direction (tetragonal) or the [200] direction (orthorhombic or monoclinic) as the film growth progressed. A similar departure from a preferential orientation was observed in CuPc films at a thickness of approximately 100 nm [40,41]. Further growth had the effect of randomizing the orientation of the phthalocyanine crystallites. Measurements of the peak width at half maximum intensity allowed an estimate of the typical microcrystallite size to be derived using the Scherrer expression. The value of 28.8 nm obtained was reasonably consistent with values of 14.7 nm [32] for ZnPc and 50–100 nm [34] for ZnPc and NiPc. A typical microcrystallite size of 10–30 nm was also determined by transmission electron microscopy in  $\alpha$ -form films of thickness 40 nm; although less than estimates obtained by the Scherrer method for films of thickness 100 nm, this is consistent with an increase in mean crystallite size with increasing film thickness. This effect has recently been definitively observed in CoPc films [42]. After annealing of  $\alpha$ -form CuPc films for 3 h at approximately 240 °C, X-ray diffraction measurements revealed a phase transition to the stable  $\beta$  form as observed previously [24,30]. A strong preferential orientation in the [20 $\bar{1}$ ] direction was evident for films of thickness 0.8  $\mu\text{m}$ , which in the  $\alpha$  form were beginning to depart from their preferred orientation; this direction has been well known since the time of Robertson's [20] work to correspond to one of the two major developed faces in  $\beta$ -CuPc crystals. Mohammed and Collins [43] have similarly observed the  $\alpha$  to  $\beta$  phase transition in CuPc films using differential scanning calorimetry. The transition was shown to be a two-stage process, with the first being exothermic and associated with growth of  $\alpha$ -phase crystals in the form of randomly orientated microcrystallites, and the second also exothermic but associated with transformation into the  $\beta$  phase and the formation of needle-like crystallites. The X-ray diffraction designations of  $\alpha$  form for films deposited at room temperature and  $\beta$  form for the evaporant and annealed films was confirmed by comparison of their IR absorption spectra with those of previous work [24,30]. These also indicated that total conversion of the films to the stable  $\beta$  form had not occurred, as also proposed for the case of H<sub>2</sub>Pc films by Sharp and Miller [44].

Shihub and Gould [42] made a similar X-ray structural study of CoPc films with particular emphasis placed on preferred orientation, mean crystallite size and the dependence of the dominant interplanar spacing on the annealing temperature. The evaporant powder was  $\beta$  form and was indexed using the lattice parameters determined by Williams et al. [36] using neutron diffraction. As with CuPc  $\alpha$ -form films [39], for a thickness of 0.1  $\mu\text{m}$  a strong preferred orientation in the [001] direction (tetragonal) or the [200] direction (orthorhombic or monoclinic) was observed, while for thicker films diffraction peaks in the range  $22^\circ < 2\theta < 28^\circ$  appeared.

However, in the case of CoPc films there was no apparent diminution in the intensity of the first peak, as is very clearly evident in Fig. 2 for CuPc films, and the intensity of the peaks at the higher angles remained relatively low. Thus the transition from the strong preferred orientation is considerably less evident in CoPc than in CuPc films for thicknesses up to 1  $\mu\text{m}$ . It was found necessary to subject the  $\alpha$ -form films of thickness 0.1  $\mu\text{m}$  to heat treatment at 300  $^{\circ}\text{C}$  before there was an almost complete phase transition to the  $\beta$  form, as observed in CuPc films [24,30,39]. However, for CuPc films the resulting preferential orientation was in the [001] direction, in contrast with that of the [201] direction for CuPc films [39]. Although these two crystallographic directions are the most highly developed in  $\beta$ -form CuPc crystals [20], the mechanism which determines the preferred orientation in  $\beta$ -form films remains unclear. However, it may be related to the existing preferential orientation in the  $\alpha$ -form films prior to the change of phase. The work referred to for CuPc films was concerned mainly with those of a thickness such that the preferential orientation in the [001] or [200] directions was not strong, particularly compared with that for CoPc films. In contrast, for CoPc the preferred orientation was still strong, even for films of thickness 1  $\mu\text{m}$ , and for the thinner films of the phase change studies there no peaks were reported other than that corresponding to the preferred orientation. Thus in the case of the CoPc films the phase change probably reflects a transition of highly oriented  $\alpha$ -phase films into highly oriented  $\beta$ -phase films. In CuPc the energetics of the process are presumably such that the moderately oriented  $\alpha$ -phase films transferred to  $\beta$ -phase films whose preferred orientation is weak, and reflect a randomization in orientation of the larger crystallites. Only a detailed X-ray study of the  $\alpha$  to  $\beta$  phase transition in different metal-substituted phthalocyanines as a function of thickness will determine whether the resulting orientation in the  $\beta$  phase is primarily a thickness-dependent effect, or whether the species of the central metal atom in the phthalocyanine molecule is more important.

A series of experiments was carried out on thin CoPc films which retained their preferential orientation on transforming from the  $\alpha$  to the  $\beta$  phase [42]. The microcrystallite grain size  $L$  was obtained using the Debye–Scherrer method on the first Bragg peak before annealing. The films were then heated to a higher temperature  $T_{\text{ann}}$  in oxygen-free nitrogen for 2 h and the value of  $L$  was measured again. Measurements were repeated at even higher temperatures until the dependence of  $L$  on  $T_{\text{ann}}$  over the entire temperature range of the phase change was determined. It was clear that at temperatures up to 200  $^{\circ}\text{C}$  there was an increase in the mean microcrystallite size from about 30 nm to over 40 nm, but no indication of a phase change. Ashida et al. [25] ascribed this effect in CuPc to preliminary crystallite growth at the early stages of the phase transformation process. Above annealing temperatures of about 200  $^{\circ}\text{C}$  there was a rapid increase in crystallite size to about 100 nm at 315  $^{\circ}\text{C}$ ; similar behaviour has also been observed in which  $\alpha$ -form CuPc films were heated to 300  $^{\circ}\text{C}$  when the diffraction patterns became sharper and the crystallites larger [25]. The  $\alpha$  to  $\beta$  phase change behaviour was also observed by carefully monitoring the values of the angle  $2\theta$  (twice the Bragg angle) for the first significant Bragg peak and the corresponding values of interplanar spacing  $d_{hkl}$ . This behaviour is illustrated in Fig. 3.  $d_{hkl}$  increased slightly with annealing temperature



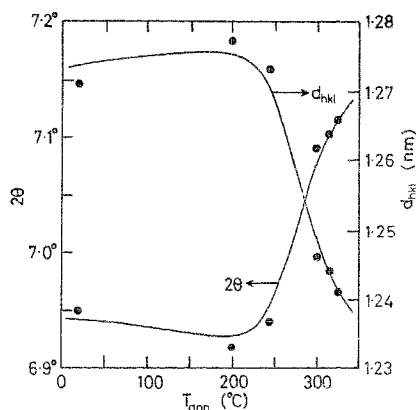


Fig. 3. Dependence of angle  $2\theta$  and interplanar spacing  $d_{hkl}$  for the first X-ray Bragg peak on the annealing temperature  $T_{\text{ann}}$  for a CoPc film of thickness 0.1  $\mu\text{m}$ . The values indicate a gradual  $\alpha$  to  $\beta$  phase transition in the temperature range 250–300°C. Reproduced with permission from Ref. [42].

up to 200°C, and then decreased significantly at 250–300°C. The value of  $2\theta$  decreased slightly with  $T_{\text{ann}}$  up to 200°C, again followed by a significant increase at approximately 250–300°C. For  $T_{\text{ann}}$  up to 250°C,  $d_{hkl}$  lay in the range 1.271–1.277 nm and  $2\theta$  in the range 6.92°–6.95°, close to the values expected for  $\alpha$ -form CoPc; at higher annealing temperatures  $d_{hkl}$  was in the range 1.241–1.246 nm and  $2\theta$  was in the range 7.09–7.12°, in better agreement with the values expected for  $\beta$ -form CoPc. A comparable decrease in  $d_{hkl}$  from 1.279 nm [23] to 1.242 nm [20] in going from the  $\alpha$  to the  $\beta$  phase is evident for CuPc, and was observed by Lucia and Verderame [45] for several phthalocyanines (including CoPc) after heat treatment at 300°C for several hours. Later work [42] confirmed that the films remain essentially of the  $\alpha$  form for  $T_{\text{ann}}$  up to approximately 250°C, but that after annealing at 300°C they transform primarily to the stable  $\beta$  form. Additional evidence for the change in structure with annealing was provided by observation of intensity profiles of the first Bragg peak, where elements of both the  $\alpha$  and  $\beta$  forms were observed for an intermediate annealing temperature of 245°C. Further evidence for the simultaneous co-existence of both phases was provided by Fryer [46], who observed electron microscopy images of both phases in  $\text{H}_2\text{Pc}$  films and also found evidence for a martensitic transformation.

Collins et al. [47] used X-ray diffraction to identify the phases of PbPc thin films evaporated onto substrates maintained at 323, 533 and 583 K (50, 260 and 310°C respectively). In agreement with earlier work from the same group [48], the films deposited at 323 K were identified as having monoclinic structure while those deposited at the higher temperatures had triclinic structure. Unlike the majority of the metal phthalocyanines, the PbPc molecule is non-planar. The central Pb atom, which is of relatively large atomic radius, is forced outside the plane containing the four isoindole rings and the four benzene rings of the molecule. The molecule then assumes

the shape of a “shuttlecock” [14], and in the monoclinic structure the shuttlecock-shaped molecules stack linearly, forming a molecular column parallel to the *c* axis. There are three possible arrangements of the molecular columns in the crystal, but according to the systematic appearances and absences of sharp reflections it was determined that the actual stacking of the molecules was such that the next-nearest-neighbour columns have the opposite sense (i.e. the Pb atom is above rather than below the molecular plane, and vice versa). This arrangement results in a monoclinic structure with  $a = 2.548$  nm,  $b = 2.548$  nm,  $c = 0.373$  nm and  $\gamma = 90^\circ$ . It was not until 1982 that the triclinic structure was determined by Iyechika et al. [15]. The lattice parameters for this structure were reported as  $a = 1.3123$  nm,  $b = 1.6131$  nm,  $c = 1.2889$  nm,  $\alpha = 94.22^\circ$ ,  $\beta = 96.20^\circ$  and  $\gamma = 114.19^\circ$ , with the PbPc molecules stacking along the *a* axis orienting their convex and concave sides alternately. For thin films deposited at 323 K, the X-ray diffraction patterns reported by Collins et al. [47] showed a weak peak corresponding to the (001) reflection with interplanar spacing 0.128 nm, consistent with a dominant monoclinic PbPc structure. The films deposited at the higher temperatures showed an intense (001) peak with interplanar spacing 0.124 nm. The weak reflection for the monoclinic structure diffraction patterns was explained as the result of the existence of two substructures with opposite orientations, while the strong peak for the triclinic structure was consistent with a high degree of crystallization. Although this recent work has not yet been confirmed, it certainly appears that the PbPc molecular phase structure can be controlled by varying the substrate temperature during deposition. Single crystals of monoclinic PbPc were grown at approximately 523 K and triclinic crystals at about 593 K [15], whereas for thin films the monoclinic structure was grown at 323 K and the triclinic at 533 K and 583 K [47]. The difference in the growth temperatures for the two phases when grown as single crystals and as thin films is an area which requires some additional investigation.

Therefore there have been some advances in the structural characterization of various phthalocyanine thin films, particularly in the last 3 years. CuPc and CoPc show thickness-dependent orientation effects and transform from the  $\alpha$  to  $\beta$  forms on annealing [39,42], while the anomalous PoPc molecule results in the growth of either the monoclinic or triclinic forms depending on the substrate temperature during deposition [47]. Clearly, further work is necessary to characterize fully the growth and phase transformation processes of these molecular thin film structures, building on these recent advances. Perhaps electrical monitoring of phase changes, of the type performed by Wihksne and Newkirk [19] for  $\alpha$ -form  $H_2$ Pc compressed powders, would be a suitable technique. This may be particularly sensitive in the case of PbPc films, since the reported room temperature conductivities of PbPc are  $10^{-2} \text{ S m}^{-1}$  in the monoclinic form [15,49] and only  $10^{-10} \text{ S m}^{-1}$  in the triclinic form [50].

### 3. Dc electrical properties

Various examples of electronic conduction processes observed in phthalocyanine thin films will be described in this section. One of the major considerations for

organic thin films is whether energy-band-type models of conductivity are applicable. This question has been addressed generally by Gutmann and Lyons [51] and more recently by Ahmad and Collins [52], the latter in the context of conductivity in triclinic PbPc films. A common rule of thumb in this regard is the use of a mobility value of  $10^{-4} \text{ m}^2 \text{ V}^{-1} \text{ s}^{-1}$ , above which band theory is considered applicable and below which hopping-type conductivity is more appropriate. However, Ahmad and Collins have argued that very low mobility values, in their case of the order of  $10^{-10} \text{ m}^2 \text{ V}^{-1} \text{ s}^{-1}$ , give an electron mean-free path orders of magnitude smaller than the i termolecular distance, and that commonly quoted arguments related to the relative validity of band and hopping models are not directly relevant. Several workers have observed values for various quantities which appear realistic by the application of a band model, and in view of this fact such models have not been ruled out in the context of low mobility values.

It is evident that phthalocyanine films prepared in a sandwich configuration between metallic electrodes can experience a considerable electric field when even relatively low voltages are applied. For example, a film of thickness  $1 \mu\text{m}$  subjected to a voltage of only 10 V experiences an average electric field of  $10^7 \text{ V m}^{-1}$ . Simmons [53] has reviewed several high-field conduction mechanisms in the context of thin dielectric films. Many of these processes have also been observed in phthalocyanine thin films and therefore they will be briefly discussed below from this point of view.

Simmons [53] has also made the important point that the type of electrode used can greatly influence the conduction processes observed, and has divided the various conduction mechanisms into bulk-limited and electrode-limited classes. In bulk-limited conductivity the charge carriers are generated in the bulk of the material and the role of the electrodes is merely to apply a potential in order to generate a drift current. For electrode-limited conductivity the interface between the electrode and the insulator or semiconductor presents a potential barrier to charge flow, which effectively limits the current. In general, contacts can be either ohmic or blocking, with the latter sometimes being known as a Schottky barrier. In ohmic contacts the energy band bending at the interface with the electrode is such that there is a reservoir of charge residing in the region of the contact, which is termed an accumulation region. This charge reservoir is capable of supplying carriers to the material as required by the bias conditions. Conversely, for blocking contacts a depletion region is formed and carriers are required to overcome a potential barrier between the Fermi level in the metal contact and the conduction or valence band edges in the insulator or semiconductor. The conditions for the formation of both types of contact are given by Simmons, although the reader should also be aware that simple considerations in terms of the relative values of the work function of the contact and of the insulator or semiconductor are rarely adequate for predicting the type of contact formed because of the frequent existence of surface states. These are usually due to the effects of unsaturated bonds and impurities at the interface [54], and can seriously alter the shape and height of the interfacial barrier. A discussion of these effects is outside the scope of this review, but the general type of contact should be recognized when considering the various conduction mechanisms described below. This section will commence with a brief discussion of the conduction processes

observed in phthalocyanine thin films, giving the relevant basic equations and the dependence of current density (or current) on voltage and/or temperature in each case, after which a summary of the results obtained for each type will be presented. The SI system of units will be used throughout, except for quantities which are almost universally expressed in other units such as those which include the electron volt (eV) rather than the SI joule as a unit of energy.

### 3.1. Basic conduction processes

Space-charge-limited conductivity (SCLC) is undoubtedly the most important conduction process in phthalocyanine thin films, having been observed in many different materials. SCLC occurs only when the injecting electrode is an ohmic contact, and therefore a reservoir of charge is available. At low voltages the thermally generated carrier concentration exceeds the injected concentration, and the current density  $J$  is given by a form of Ohm's law

$$J = p_0 e \mu \frac{V}{d} \quad (1)$$

where  $p_0$  is the thermally generated carrier concentration (holes in the case of most phthalocyanines which are generally  $p$  type),  $e$  is the electronic charge,  $\mu$  is the mobility (again normally for holes),  $V$  is the applied voltage and  $d$  is the film thickness. When ohmic contacts are applied majority carriers may be injected into the material, and when the injected carrier concentration exceeds that of the thermally generated concentration the SCLC current becomes dominant. However, the existence of traps within imperfect extrinsic materials has the effect of immobilizing a large proportion of the injected carriers. If the traps are shallow and located at a discrete energy  $E_t$  above the valence band edge, the SCLC is given by

$$J = \frac{9}{8} \epsilon_r \epsilon_0 \theta \mu \frac{V^2}{d^3} \quad (2)$$

where  $\epsilon_r$  is the relative permittivity of the material,  $\epsilon_0$  is the permittivity of free space and  $\theta$  is the ratio of free to trapped charge. In Eq. (2) we have not followed Lampert [55] in omitting the constant  $9/8$  on the right-hand side of the expression. The quantity  $\theta$  is described by [7]

$$\theta = \frac{N_v}{N_{t(s)}} \exp\left(-\frac{E_t}{kT}\right) \quad (3)$$

where  $N_v$  is the effective density of states at the valence band edge,  $N_{t(s)}$  is the trap concentration residing in the discrete energy level,  $k$  is Boltzmann's constant and  $T$  is the absolute temperature. It is clear that there is a transition between the two conduction mechanisms described by Eqs. (1) and (2), which occurs at a transitional voltage  $V_t$  when the injected carrier concentration first exceeds the thermally gener-

ated carrier concentration. This voltage has the form

$$V_t = \frac{8ep_0d^2}{9\theta\epsilon_r\epsilon_0} \quad (4)$$

However, a single shallow trap level is frequently replaced by an exponential distribution of traps  $P(E)$  described by the relationship

$$P(E) = P_0 \exp\left(-\frac{E}{kT_t}\right) \quad (5)$$

where  $P(E)$  is the trap concentration per unit energy range at an energy  $E$  above the valence band edge,  $P_0$  is the value of  $P(E)$  at the valence band edge and  $T_t > T$  is a temperature parameter characterizing the distribution. It can be shown that the total concentration  $N_{(te)}$  of traps comprising the distribution is [56]

$$N_{(te)} = P_0 k T_t \quad (6)$$

and the current density is given by [55]

$$J = e\mu N_v \left( \frac{\epsilon_r \epsilon_0}{e P_0 k T_t} \right)^l \frac{V^{l+1}}{d^{l+1}} \quad (7)$$

This expression predicts a power-law dependence of  $J$  on  $V$  with the exponent  $n = l + 1$ , where  $l$  represents the ratio  $T_t/T$ . Analogously to Eq. (4) there is also a transition voltage between ohmic conduction and SCLC dominated by an exponential trap distribution; in this case the transition voltage is given by [57]

$$V_t = \left( \frac{p_0}{N_v} \right)^{1/l} \frac{e P_0 k T_t d^2}{\epsilon_r \epsilon_0} \quad (8)$$

On the basis of these expressions for SCLC dominated by an exponential trap distribution, Gould [58] showed that measurements of  $J$  as a function of temperature at constant applied voltage in the SCLC region could be used to determine the mobility and trap concentration. If the data are plotted in the form  $\log_{10} J$  against  $1/T$  the curves should be linear, and when extrapolated to negative values of  $1/T$  they should all intersect at a common point irrespective of applied voltage. The coordinates of this point are given by

$$\log_{10} J = \log_{10} \left( \frac{e^2 \mu d N_v N_{(te)}}{\epsilon_r \epsilon_0} \right) \quad \frac{1}{T} = -\frac{1}{T_t} \quad (9)$$

The slopes of the lines are

$$\frac{d(\log_{10} J)}{d(1/T)} = T_t \log_{10} \left( \frac{\epsilon_r \epsilon_0 V}{e d^2 N_{(te)}} \right) \quad (10)$$

and the intercept  $\log_{10} J_0$  on the  $\log_{10} J$  axis is given by

$$\log_{10} J_0 = \log_{10} \left( \frac{e\mu N_v V}{d} \right) \quad (11)$$

This set of equations has been used to determine mobility and trap concentration in various materials showing this form of SCLC, and in particular in thin films of phthalocyanines, for example CuPc [59] and the triclinic form of PbPc [60]. All of the above discussion on SCLC has been concerned with single carrier injection; this is the situation when only one type of carrier is injected in appreciable numbers. The effect of double injection, when one electrode is ohmic for electrons and the other is ohmic for holes, has not to the author's knowledge been identified in phthalocyanine thin films. However, a very detailed description of this phenomenon is given in the standard text by Lampert and Mark [61] on current injection in solids, while Lamb [54] also provides a useful description.

A second bulk-limited conduction process is the Poole–Frenkel effect. The effect is often referred to as the bulk analogue of the Schottky effect, a well-known electrode-limited process, which is itself covered below. In essence the Poole–Frenkel effect is the field-assisted lowering of the coulombic potential barrier between carriers at impurity levels and the edge of the conduction or valence bands. When a carrier is trapped at a centre, it is unable to contribute to the conductivity until it overcomes a potential barrier  $\phi$  and is promoted into one of the free bands. In the presence of a high electric field the potential is reduced by an amount  $eFx$  where  $e$  is the electronic charge,  $F$  is the applied field and  $x$  is the distance from the centre. This results in a lowering of the potential barrier by an amount  $\Delta\phi_{PF}$  which depends on the electric field according to the relationship

$$\Delta\phi_{PF} = \beta_{PF} F^{1/2} \quad (12)$$

where

$$\beta_{PF} = \left( \frac{e^3}{\pi\epsilon_r\epsilon_0} \right)^{1/2} \quad (13)$$

is the Poole–Frenkel field-lowering coefficient. (The SI unit for this quantity is  $\text{J m}^{1/2} \text{V}^{-1/2}$ , although it is customarily quoted in a unit of  $\text{eV m}^{1/2} \text{V}^{-1/2}$ ). The current density then follows the relationship

$$J = J_0 \exp \left( \frac{\beta_{PF} F^{1/2}}{kT} \right) \quad (14)$$

where  $J_0 = \sigma_0 F$  is the low-field current density. Although this is the form of the equation normally used in thin-film work, owing to the almost universal presence of traps, if the low-field conductivity  $\sigma_0$  shows an intrinsic dependence and is proportional to the factor  $\exp(-E_G/2kT)$  where  $E_G$  is the energy gap, then a factor of 2 would appear in the denominator of the exponential term of Eq. (14). Although  $J_0$  in this equation depends on  $F$ , the variation is considerably less than that of the

exponential term and is frequently ignored in comparison. Since  $F = V/d$ , Eq. (14) can be rewritten as

$$J = J_0 \exp\left(\frac{\beta_{\text{PF}} V^{1/2}}{k T d^{1/2}}\right) \quad (15)$$

Thus a linear plot of  $\log J$  against  $V^{1/2}$  should be obtained, from which a value of the field-lowering coefficient can be obtained and compared with the theoretical value predicted by Eq. (12). If the variation of the pre-exponential factor is also to be taken into account, then a linear plot of  $\log(J/V)$  against  $V^{1/2}$  should be obtained.

Several modified versions of Eq. (14) have been suggested to account for the current density variation in the presence of various combinations of centres such as donors and traps; a particular example of one of these is given by Simmons [53]. More recently, Gould and Bowler [62] have proposed the following expression for the dependence of Poole–Frenkel conduction, in which the electric field is non-uniform and has a maximum value of  $\alpha^2 F$ , where  $F$  is the mean field

$$J = \frac{2J_0 k T}{\alpha \beta_{\text{PF}} F^{1/2}} \exp\left(\frac{\alpha \beta_{\text{PF}} F^{1/2}}{k T}\right) \quad (16)$$

Interpretations of results in terms of this expression have been made for CuPc [63] and PbPc [13] thin films.

A third bulk-limited conduction process, which has been claimed to have been observed in thin films of (FePc)K (iron phthalocyanine co-evaporated with potassium) [64], and later in triclinic PbPc [52], is known as hopping. This general process is well known in non-crystalline materials, and is described in various standard texts covering this area [65,66]. In such materials the lack of long-range order gives rise to a phenomenon known as localization, in which the energy levels do not merge into one another, particularly in the region of the edges of the energy bands (band tails). The effect of this is that in order for carriers to be transported through the material and to contribute to the conductivity they have to proceed by a series of jumps or “hops” from one localized energy level to another. Hopping occurs between the various localized energy levels when energy (usually thermal) is available. However, since the localized levels are normally very close in energy, the thermal energy required is very small and therefore the process can occur at very low temperatures when other conduction processes are precluded. According to Mott and Davis [66], in this type of material the conductivity  $\sigma$  exhibits different behaviour in different regions of its  $\log \sigma$  versus  $1/T$  characteristic. At higher temperatures thermal excitation of carriers to the band edges is possible and extended-state conductivity can take place, while at lower temperatures, where less thermal energy is available, hopping may occur. There are various different hopping regimes, for instance the self-explanatory nearest-neighbour hopping and variable-range hopping. In the latter process hopping takes place to a more distant neighbour, where the energy difference between the states is lower. For variable-range hopping the conduc-

tivity is expected to follow a relationship of the type [65]

$$\sigma = \sigma_0 \exp\left(-\frac{A}{T}\right)^{1,4} \quad (17)$$

where  $\sigma_0$  and  $A$  are constants. A plot of  $\log \sigma$  versus  $T^{-1/4}$  should then be linear with negative slope.

Of the electrode-limited conduction processes, tunnelling is normally applicable only for very thin films of thickness less than about 10 nm when subjected to a high electric field. Therefore, it has not generally been observed in phthalocyanines, owing to the thicker films which are usually used. Tunnelling is a quantum-mechanical effect in which the wave function of the carrier is attenuated only moderately by the thin barrier, so that the carrier has a finite probability of existence on the opposite side of the barrier. Simmons [53] has reviewed the tunnelling process in some detail under a wide variety of conditions of applied voltage and work function values. In particular, it has been proposed [67] that a modified Fowler–Nordheim expression may be applicable for tunnelling through an interfacial region of thickness  $d_t$ , where the electric field at the barrier is sufficiently high to reduce its width, measured at the Fermi level, to about 5 nm. Under these circumstances the current density is related to the voltage and barrier thickness by the expression

$$J = \frac{e^3 V^2}{8\pi h \phi d_t^2} \exp\left(-\frac{8\pi(2m)^{1/2} \phi^{3/2} d_t}{3ehV}\right) \quad (18)$$

where  $h$  is Planck's constant,  $\phi$  and  $d_t$  are the barrier height and effective thickness respectively of the tunnelling barrier and  $m$  is the mass of the free electron.

The Schottky effect is the field-assisted lowering of a potential barrier at the injecting electrode and, as mentioned above, is conceptually similar to the Poole–Frenkel effect. This type of conduction process occurs when the film is too thick for tunnelling to take place. The potential barrier at the metal/semiconductor interface is reduced by an amount  $\Delta\phi_s$ , which is given by

$$\Delta\phi_s = \beta_s F^{1/2} \quad (19)$$

where

$$\beta_s = \left(\frac{e^3}{4\pi\epsilon_r\epsilon_0}\right)^{1/2} \quad (20)$$

is the Schottky field-lowering coefficient. By comparison with Eq. (13), it is clear that  $\beta_{PF} = 2\beta_s$ . Richardson's basic thermionic emission equation

$$J = AT^2 \exp\left(-\frac{\phi}{kT}\right) \quad (21)$$

predicts the current density flowing via emission of carriers over a potential barrier of height  $\phi$  at a temperature  $T$ .  $A$  is the Richardson constant, which has a theoretical value of  $1.2 \times 10^6 \text{ A m}^{-2}$ . Note that the current density depends only on the barrier



height and the temperature, and does not depend explicitly on the applied voltage. If  $\phi_0$  is the zero-voltage barrier height, then the reduced barrier height  $\phi$  is given by  $(\phi_0 - \Delta\phi_s)$  so that Eq. (21) yields

$$J = AT^2 \exp\left(-\frac{\phi_0}{kT}\right) \exp\left(\frac{\beta_s F^{1/2}}{kT}\right) \quad (22)$$

or

$$J = AT^2 \exp\left(-\frac{\phi_0}{kT}\right) \exp\left(\frac{\beta_s V^{1/2}}{kTd^{1/2}}\right) \quad (23)$$

Thus in principle the Schottky and Poole–Frenkel effects can be distinguished by the measured value of the field-lowering coefficient, which is twice as high in the Poole–Frenkel case as in the Schottky case.

Finally, diode-type conductivity may also be observed in phthalocyanines. The Schottky effect described above corresponds to the flow of carriers across a metal–semiconductor interface under reverse bias, when the dominant effect controlling the form of the current is field-lowering of the Schottky barrier [68]. However, if the voltage is applied in the opposite (or forward) direction, the current density increases according to the diode equation

$$J = J_s \left[ \exp\left(\frac{eV}{\eta kT}\right) - 1 \right] \quad (24)$$

where  $J_s$  is the reverse saturation current density given by

$$J_s = A^{**} T^2 \exp\left(-\frac{\phi_b}{kT}\right) \quad (25)$$

where  $A^{**}$  is the effective Richardson constant,  $\phi_b$  is the barrier height and  $\eta$  is the diode quality (or ideality) factor, which is introduced to allow for carrier recombination effects [69]. Obviously, for a sample with two metal electrodes contacting the two sides of a phthalocyanine film, there are two metal–semiconductor junctions. Generally one of these effectively dominates the conductivity, and it is whether this junction is forward- or reverse-biased that determines the form of the conductivity.

This section has attempted to cover most of the dc conduction processes observed to date in phthalocyanine films, examples of all of which are given in the following sections. It should be noted that, in many structures, significant differences can be observed depending on the polarity, the magnitude of the applied voltage and the temperature. Thus in the work described below these features have normally been taken into account. It should also be noted that in many cases it is very difficult to distinguish between, for example, SCLC and the Poole–Frenkel effect on the basis of current density–voltage characteristics alone, and that distinguishing between the Poole–Frenkel and Schottky effects is notoriously difficult.

### 3.2. Space-charge-limited conductivity

Delacote et al. [70] made early electrical measurements on Au|CuPc|Au sandwich structures, and observed an ohmic region followed by an exponential and then a square-law dependence of current on voltage. They concluded that at low voltages conduction was by a thermally activated hole current, whereas in the exponential region SCLC took place, dominated by a uniform distribution of traps as described by Rose [7]. Following this, Sussman [9] made an extensive series of measurements on the same system, both in the dark and under illumination, and from these measurements was able to prove conclusively that SCLC, dominated by an exponential hole trap distribution, was responsible for the conduction behaviour. In Fig. 4 Sussman's results are shown for a sample with CuPc thickness approximately 0.2  $\mu\text{m}$ , at various temperatures from 210 K to 430 K. All samples showed ohmic conductivity at low voltages (slope 1) and this was followed by SCLC. The limiting slope values are indicated on the figure. Sussman pointed out that as the sample temperature  $T$  increases, the value of the slope should decrease, since it is given by  $(T_i + T)/T$  where  $T_i$  is the temperature parameter describing the trap distribution (see Eqs. (5) and (7)). Sussman also observed an inverse power law of current on thickness, as predicted by Eq. (7). Furthermore, he established that a set of double-logarithmic plots of

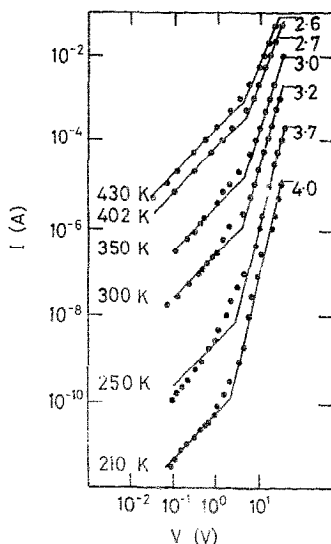


Fig. 4. Current-voltage ( $I$ - $V$ ) characteristics of a Au|CuPc|Au sample at different temperatures, showing ohmic conductivity followed by SCLC. The limiting slope is indicated for each characteristic, and decreases with increasing temperature as predicted by Sussman. Adapted with permission from Ref. [9].

current versus voltage for SCLC dominated by an exponential trap distribution should all be linear and should intersect at a common point whose coordinates could be used in the calculation of parameters such as mobility and trap concentration. Since Sussman's paper was first published, SCLC dominated by both discrete trap levels (Eqs. (2)–(4)) and exponential trap distributions (Eqs. (5)–(8)) has been identified in many phthalocyanine thin-film materials. A summary of the results obtained from a selection of this work, using various different electrodes is given in Table 1. In this table results for samples where oxygen or other gases have been deliberately introduced, thus varying the trap concentration, have generally been omitted; in particular a considerable quantity of data derived by Ahmad and Collins [52] for PbPc under different oxygen storage and annealing conditions has not been included. When the data for fresh samples are not provided, values for the shortest storage times are given.

It is clear that the values of thermally generated hole concentration  $p_0$  are normally between  $10^{16}$  and  $10^{18} \text{ m}^{-3}$  for films which have not been annealed, with the exception of CuPc films having indium electrodes [72]. If extremely low mobility values are not adopted for this configuration, the low value suggests that carrier compensation effects in the vicinity of the electrode are probable. Total trap concentrations for exponential distributions span a wide range from  $6 \times 10^{20}$  to  $9.3 \times 10^{26} \text{ m}^{-3}$ . However, this variation is believed to be dependent on the phthalocyanine purity, preparation conditions, phase, thermal history and electrode materials. When discrete trap level SCLC is considered, the range of trap concentrations reported is from  $5 \times 10^{16}$  to  $7.1 \times 10^{25} \text{ m}^{-3}$ . However, the highest value is exceptional [13,76], having been derived for PbPc assuming a high reported mobility of  $3.7 \times 10^{-4} \text{ m}^2 \text{ V}^{-1} \text{ s}^{-1}$  [81]. More recently, a mobility value of only  $6.05 \times 10^{-10} \text{ m}^2 \text{ V}^{-1} \text{ s}^{-1}$  has been reported [60]. The assumption of a lower mobility value might mitigate this discrepancy. Otherwise the trap concentrations in the single-level mode vary in the narrower range of  $5 \times 10^{16}$  to  $3.5 \times 10^{19} \text{ m}^{-3}$ . Traps distributed exponentially in energy appear able to accommodate higher overall trap concentrations. Activation energies for discrete trap levels have been reported as 0.62 eV [73] and 0.77 eV [74] in CuPc, 0.42 eV in PbPc [13,76], 0.58 eV in NiPc [78,79], and 0.45 eV (fresh) and 0.69 eV (annealed) in CoPc [80]. Therefore there appears to be some difference in this value between the various phthalocyanines, which is probably a function of the central metal atom in the molecule and possibly the oxygen content.

It has been well established that oxygen doping increases the conductivity of phthalocyanine thin films and that annealing drives out the oxygen, thus lowering the conductivity. In CuPc films [73] exposure to oxygen increased the value of  $p_0$  from  $5 \times 10^{17} \text{ m}^{-3}$  after storage for 2 weeks to  $10^{20} \text{ m}^{-3}$  after storage for 20 weeks. Annealing reduced its value to  $1.9 \times 10^{14} \text{ m}^{-3}$ . A similar, but less drastic, effect has also been observed by Ahmad and Collins [52] in PbPc films, which showed a  $p_0$  value of  $2.2 \times 10^{18} \text{ m}^{-3}$  after storage for 2 weeks,  $4.5 \times 10^{19} \text{ m}^{-3}$  after storage for 25 weeks and  $1.4 \times 10^{18} \text{ m}^{-3}$  after annealing. Twarowski [82,83] mentioned that oxygen outgassing might occur in ZnPc. Furthermore, it is known that the transition from the  $\alpha$  to the  $\beta$  phase takes place as the temperature is increased. Twarowski suggested that the low conductivity of the  $\beta$  phase may be due in part to the deeper

Table 1

Values of the thermally generated hole concentration  $p_0$  and the total trap concentration  $N_t$  derived for various phthalocyanine sandwich structures using SCLC measurements

Configuration	$p_0$ ( $\text{m}^{-3}$ )	$N_t$ ( $\text{m}^{-3}$ )	$T_t$ (K)	$E_t$ (eV)	Reference
Au CuPc Au		$2.0 \times 10^{26}$	680		[9]
Au  $\alpha$ -CuPc Au		$6.0 \times 10^{20}$	1800		[11]
Au  $\beta$ -CuPc Au		$6.0 \times 10^{21}$	1700		[11]
Au CuPc Au	$9.1 \times 10^{17}$	$4.0 \times 10^{23}$	750		[71]
Au CuPc Au		$5.0 \times 10^{22}$ – $6.0 \times 10^{24}$	750		[59]
In CuPc In	$5.0 \times 10^{14}$	$7.5 \times 10^{23}$	1421		[72]
(type A)					
In CuPc In	$1.8 \times 10^{17}$	$4.3 \times 10^{24}$	781		[72]
(type B)					
Au  $\alpha$ -CuPc Au	$3.0 \times 10^{17}$	$7.3 \times 10^{18}$		0.62	[73]
(2 weeks)					
Au CuPc Au	$1.9 \times 10^{14}$	$1.5 \times 10^{24}$	816		[73]
(annealed)					
Au CuPc Al		$2.0 \times 10^{22}$	885		[63]
Ar CuPc Al		$3.5 \times 10^{19}$		0.62	[63]
Au CuPc Au	$4.0 \times 10^{17}$	$1.0 \times 10^{24}$	767		[74]
Au(t) CuPc Pb		$1.8 \times 10^{22}$	1060		[74]
Au(t) CuPc Pb		$5.0 \times 10^{16}$		0.77	[74]
Au(t) CuPc Pb		$1.0 \times 10^{24}$	767		[74]
Au(b) CuPc Pb		$4.4 \times 10^{22}$	1060		[74]
Au(b) CuPc Pb		$8.0 \times 10^{18}$		0.77	[74]
Au(b) CuPc Pb		$2.4 \times 10^{25}$	767		[74]
Ag H <sub>2</sub> Pc Ag	$1.2 \times 10^{15}$	$1.0 \times 10^{22}$			[33]
Au PbPc Au	$(1.1-2.1) \times 10^{10}$	$(2.1-8.0) \times 10^{25}$	(586-665)		[75]
Au PbPc Al		$7.6 \times 10^{24}$	776		[13.76]
Au PbPc Al		$7.1 \times 10^{25}$		0.42	[13.76]
Au PbPc Au	$1.6 \times 10^{18}$	$3.0 \times 10^{23}$	770		[60]
Au NiPc Au	$3.2 \times 10^{15}$	$2.9 \times 10^{22}$	1823		[77]
	$3.4 \times 10^{17}$				
Au NiPc Au	$7.2 \times 10^{18}$	$1.0 \times 10^{19}$		0.58	[78.79]
(fresh)					
Au NiPc Au	$2.3 \times 10^{14}$	$9.3 \times 10^{20}$	548		[78.79]
(annealed)					
Au  $\alpha$ -CoPc Au	$8.0 \times 10^{17}$	$1.0 \times 10^{24}$	885		[80]
(fresh)				0.45	[80]
Au CoPc Au	$3.0 \times 10^{16}$	$1.0 \times 10^{24}$	885		[80]
(annealed)				0.69	[80]

$T_t$  is the temperature parameter for an exponential trap distribution and  $E_t$  is the activation energy for traps located at a discrete energy level. For asymmetric device configurations the injecting ohmic electrode is given first: (b) indicates that this is the bottom electrode (substrate side) while (t) indicates the top (non-substrate) side.  $\alpha$  and  $\beta$  refer to the crystal structure, and in some cases details of various treatments are given (e.g. fresh, annealed, or 2 weeks (the storage time)). Types A and B for In|CuPc|In structures are defined in Ref. [72].  $p_0$  and  $N_t$  have been rounded to one decimal place.

trap levels present in that phase. A further interesting point which has emerged from recent results is that after storage in oxygen the SCLC tends to be of the square-law rather than the power-law variety, with the power-law behaviour reappearing after annealing. This has been observed in CuPc [73], CoPc [80] and PbPc [52]. Thus, after exposure to a high oxygen concentration for extended periods, the conductivity process appears to be dominated by a single level, presumably due to the oxygen, while the exponential trap distribution after annealing probably reflects the inherent conductivity of the material. Ahmad and Collins [52] also observed the reappearance of square-law behaviour after exposure of previously annealed PbPc films to an oxygen atmosphere.

Gould [59] utilized the method defined by Eqs. (9)–(11) to determine the variation of trap concentration and mobility in CuPc films as a function of both background pressure and deposition rate. The deposition rate  $R$  used in preparing the films varied from 0.1 to 5.0 nm s<sup>-1</sup>, and the background pressure  $P$  varied from  $1.3 \times 10^{-1}$  to  $1.3 \times 10^{-4}$  Pa. By exploiting the spread of these two ranges, it was possible to cover a range of  $P/R$  from  $2.6 \times 10^4$  to  $1.3 \times 10^9$  Pa m<sup>-1</sup> s. Fig. 5 shows the dependence of both mobility  $\mu$  and total trap concentration  $N_{\text{tle}}$  on  $P/R$ . There was a significant decrease in mobility and an increase in trap concentration as  $P/R$  increased. It was estimated that the ratio of the number of incident gas molecules (oxygen and nitrogen) to the number of deposited CuPc molecules was in the range  $0.4\text{--}2 \times 10^4$  for the  $P/R$  range covered. The decrease in mobility from  $10^{-6}$  to  $10^{-8}$  m<sup>2</sup> V<sup>-1</sup> s<sup>-1</sup> and the increase in the trap concentration from  $5 \times 10^{22}$  to  $6 \times 10^{24}$  m<sup>-3</sup> were ascribed respectively to additional scattering of carriers and trapping by the oxygen and nitrogen molecules incorporated in the structure. The same method was used by Ahmad and Collins [60] to derive a mobility value of  $6.05 \times 10^{-10}$  m<sup>2</sup> V<sup>-1</sup> s<sup>-1</sup> in PbPc films. Therefore the former work on CuPc estab-

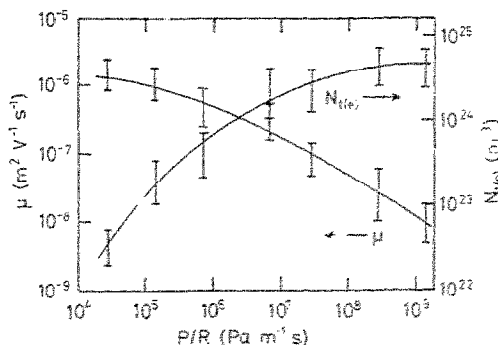


Fig. 5. Dependence of mobility  $\mu$  and total trap concentration  $N_{\text{tle}}$  for Au/CuPc/Au samples on the ratio of evaporation pressure to deposition rate  $P/R$ .  $\mu$  and  $N_{\text{tle}}$  were derived from current density-temperature measurements at constant voltage in the SCLC range using Eqs. (9)–(11). Adapted with permission from Ref. [59].

lished that there was a systematic variation of over two orders of magnitude for mobility and trap concentration, which could be directly related to the deposition conditions.

In view of the low mobility values, measurement of this quantity in phthalocyanine films is not a simple task as Hall effect measurements require the detection of very low voltages and the use of a relatively high magnetic field. The SCLC method described above, and various calculations from SCLC data, are the most frequently used techniques, although other methods such as time-of-flight measurements [84] and calculations using measurements of the Seebeck coefficient [81] have also been used. In addition to the mobility measurements described above, other measurements involving SCLC have yielded values of  $10^{-8} \text{ m}^2 \text{ V}^{-1} \text{ s}^{-1}$  [70],  $2 \times 10^{-7} \text{ m}^2 \text{ V}^{-1} \text{ s}^{-1}$  or  $2 \times 10^{-6} \text{ m}^2 \text{ V}^{-1} \text{ s}^{-1}$  (depending on the structure) [11] and  $2 \times 10^{-6} \text{ m}^2 \text{ V}^{-1} \text{ s}^{-1}$  [9] for CuPc films. Mycielski et al. [84] determined a value of  $10^{-8} \text{ m}^2 \text{ V}^{-1} \text{ s}^{-1}$  using time-of-flight measurements for CuPc films, while Laurs and Heiland [85] measured surface conductivity in several phthalocyanines and derived values of drift mobility in CuPc films spanning the range  $10^{-13}$ – $10^{-9} \text{ m}^2 \text{ V}^{-1} \text{ s}^{-1}$ . The extremely high mobility value of  $3.7 \times 10^{-4} \text{ m}^2 \text{ V}^{-1} \text{ s}^{-1}$  [8] determined for PbPc from measurements of conductivity and thermoelectric power is in complete contrast to the value of  $6.05 \times 10^{-10} \text{ m}^2 \text{ V}^{-1} \text{ s}^{-1}$  [60] obtained using SCLC measurements. The major conclusions that can be drawn from these measurements are that (i) there is a great difference in mobility values depending on the deposition conditions, although the mobility is to some extent controllable, and (ii) mobility values are, with one exception, very low and possibly outside the range of applicability of the band model [52]. Considerably more work requires to be performed on this aspect of phthalocyanine thin films, and the SCLC technique appears to offer a method which at least gives self-consistent results for a given material deposited under different conditions. Detailed mobility measurements have previously been confined mainly to CuPc and PbPc films, and their extension to other phthalocyanines would be of considerable interest.

### 3.3. The Poole–Frenkel effect

Poole–Frenkel conductivity is an effect which is normally bulk limited, i.e. the electrodes do not have an appreciable influence in determining the observed current density. However, it is not observed in phthalocyanine thin films when an ohmic contact is used, as SCLC is predominant. However, the effect has been reported in films where the injecting electrode is not ohmic, usually in the higher voltage range and accompanied by a different lower-voltage conduction process such as Schottky emission.

Poole–Frenkel conductivity in a structure incorporating CuPc was first reported by Hassan and Gould [72]. However, in this case true Poole–Frenkel conduction in the phthalocyanine layer was not observed. The structure investigated was  $\text{In}|\text{CuPc}|\text{SiO}_x|\text{In}$ , where  $1 < x < 2$ , and although the In electrode appeared to act as an ohmic contact to the CuPc, the insulating  $\text{SiO}_x$  layer effectively dominated the conductivity. The measured value of the field-lowering coefficient  $\beta$  was  $1.95 \times 10^{-5} \text{ eV m}^{1/2} \text{ V}^{-1/2}$ . Similar values have been obtained in  $\text{SiO}_x$  films by many

workers [72], and were identified with a form of Poole–Frenkel conductivity, rather than the Schottky effect, mainly because the  $\beta$  value did not depend on the electrode material [86]. However, these workers [63] did observe Poole–Frenkel conductivity in oxygen-doped CuPc films of thickness 5  $\mu\text{m}$  using one gold and one aluminium electrode. When biased with the aluminium electrode positive (injecting for holes), a linear dependence of  $\log J$  on  $V^{1/2}$  was observed. The theoretical value of  $\beta_{\text{PF}}$  for CuPc was calculated as  $4 \times 10^{-5} \text{ eV m}^{1/2} \text{ V}^{-1/2}$  from Eq. (13). For voltages in excess of about 16 V the measured value of  $\beta$  was  $6.4 \times 10^{-5} \text{ eV m}^{1/2} \text{ V}^{-1/2}$  for an oxygen-doped sample and  $2.9 \times 10^{-5} \text{ eV m}^{1/2} \text{ V}^{-1/2}$  for an annealed sample. The value obtained for the oxygen doped sample was rather higher than the usual theoretical value, but explicable in terms of a non-uniform internal electric field distribution via Eq. (16). For annealed samples the measured  $\beta$  value was reasonably close to the theoretical value and thus conventional Poole–Frenkel conductivity with a uniform electric field distribution was identified. Similarly, in Au/CuPc/Pb samples [74] Poole–Frenkel conductivity with  $\beta = 3.2 \times 10^{-5} \text{ eV m}^{1/2} \text{ V}^{-1/2}$  was observed for applied voltages above about 3 V when the Pb electrode was positively biased.

In Au/PbPc/Al structures [13,76], with the aluminium electrode positively biased, a  $\beta$  value of  $5.84 \times 10^{-5} \text{ eV m}^{1/2} \text{ V}^{-1/2}$  was obtained, compared with a theoretical value for PbPc of  $3.84 \times 10^{-5} \text{ eV m}^{1/2} \text{ V}^{-1/2}$  for the Poole–Frenkel effect. Again, this slightly higher value was identified with a possibly non-uniform electric field distribution. At lower voltages a higher  $\beta$  value was determined, which was identified as Schottky emission, but taking place over a limited range of the film thickness. Very similar results have also been reported by Ahmad and Collins [87] for this system, again showing two ranges of linear  $\log J$  versus  $V^{1/2}$  behaviour. However, in this case both were interpreted in terms of the Schottky effect but with different barrier widths, although the possibility of interpretation involving Poole–Frenkel emission was also mentioned. Additionally, Kašpar et al. [88] interpreted their results for PbPc films containing oxygen in terms of both the Poole–Frenkel and Schottky effects, although their films had two gold electrodes.

Thus there have been several reports of Poole–Frenkel conductivity in phthalocyanine thin films. Interpretations of the data have been disposed towards the Poole–Frenkel rather than the Schottky effect where the  $\beta$  values have been slightly higher than the theoretical Poole–Frenkel value but significantly in excess of the corresponding Schottky values. However, in some cases measured  $\beta$  values which greatly exceed both theoretical values have been interpreted in terms of Schottky emission over a barrier of width less than the full film thickness. Definitive measurements are clearly required in a well-defined phthalocyanine material using, for one contact, a wide range of electrode materials with different work functions. Similar electrical behaviour irrespective of electrode material under reverse bias would indicate Poole–Frenkel conductivity, while Schottky behaviour should exhibit different values of current density owing to the differing barrier heights.

### 3.4. Variable range hopping conduction

Hopping is a conduction mechanism normally associated with non-crystalline materials such as glasses. Nevertheless, it is known that phthalocyanine films occa-

sionally have an amorphous structure [33], and therefore the possibility of amorphous regions existing in nominally  $\alpha$ - or  $\beta$ -phase phthalocyanine films is not excluded.

The Mott  $T^{-1/4}$  law for variable-range hopping was tentatively identified in (FePc)K by Le Moigne and Even [64]. Basic activation energy measurements revealed a change in slope or “kink”, which implied a significant difference in activation energy of  $0.04 \pm 0.01$  eV. The existence of two different thermally activated processes in both the ohmic and SCLC conductivity ranges led to the assumption that a change in the transport mechanism occurred as a result of a change in mobility of the charge carriers. The data were plotted according to expression (17), and showed a linear dependence of  $\log \sigma$  on  $T^{-1/4}$  for a  $T^{-1/4}$  range of approximately  $0.26$ – $0.29$  K $^{-1/4}$  (140–220 K). The linearity was particularly good in the range 156–175 K and variable-range hopping was proposed as the conduction mechanism, although it was pointed out that the range of the data was too limited for a full test of the  $T^{-1/4}$  law.

More recently, work on triclinic PbPc films sandwiched between gold electrodes has also shown evidence of variable-range hopping at low temperatures [52]. In this work activation energies were measured at constant voltage (current density varied with temperature) and also by making a series of measurements at constant temperature (current density varied with voltage). Therefore in the latter series of measurements the devices were progressively annealed during the course of the measurements. A “kink” similar to that observed by Le Moigne and Even [64] was also observed in the activation energy plots and thus analysis in terms of Eq. (17) was attempted. Fig. 6 shows a plot of  $\log_{10}[J(T) - J(160\text{ K})]$  against  $T^{-1/4}$  for an applied voltage of 1 V in the ohmic range. This shows a linear variation,

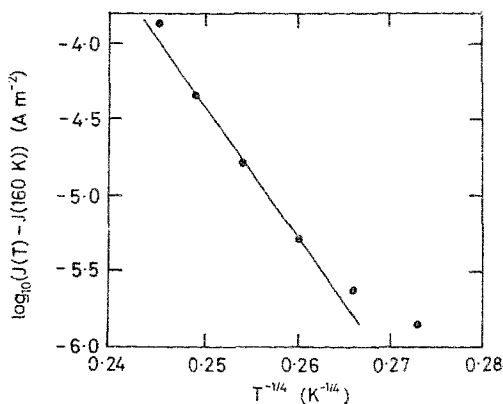


Fig. 6. Dependence of  $\log_{10}[J(T) - J(160\text{ K})]$  on  $T^{-1/4}$  for the ohmic conduction region (1 V) in a Au/triclinic PbPc/Au sample. The linear plot verifies the  $T^{-1/4}$  law of Eq. (17) for variable-range hopping. Adapted with permission from Ref. [52].



indicating that Eq. (17) is obeyed over the relevant temperature range. It should also be noted that a similar linear variation was also observed in the SCLC region, with plots similar to that of Fig. 6 presented for applied voltages of 50 and 100 V; however, in the SCLC region there was a change in slope at a temperature corresponding to approximately  $T^{-1/4} = 0.25 \text{ K}^{-1/4}$ .

The work on both (FePc)K and PbPc has shown evidence of dc variable-range hopping at reduced temperatures, although both groups of authors [52,64] stated that a full test of the  $T^{-1/4}$  law requires the acquisition of data over a wider range of temperatures. Although this is true, there is some additional recent evidence from ac measurements in several evaporated phthalocyanine materials that supports the evidence of hopping at low temperatures [89–92].

### 3.5. Tunnelling

In their electrical measurements on CuPc films using indium electrodes, Hassan and Gould [72] observed that there was a very sharp increase in current density at approximately 1 V when the bottom (substrate) electrode was biased positive, and that this was absent when the structure was biased in the opposite polarity. Furthermore, under the opposite polarity the indium electrodes appeared to act as ohmic contacts and the usual ohmic conduction followed by SCLC was observed. It had previously been suggested [12] that oxidation of indium contacts during deposition may take place and that tunnelling through this layer might occur. It was estimated [72] that the impingement rate of oxygen molecules in the vacuum chamber under the conditions of deposition was of the order of  $5.4 \times 10^{17} \text{ m}^{-2} \text{ s}^{-1}$ , allowing oxidation of the bottom electrode between the cessation of its deposition and the commencement of the deposition of the CuPc film. Although the oxide layer was considered unlikely to exceed a thickness of 1.5 nm, and thus was unlikely to dominate the overall conductivity by itself, it was proposed that the presence of such a layer may serve to modify the electronic character of the In|CuPc contact such that tunnelling into the valence band could occur over a rather greater thickness.

Simmons [67] had proposed that a modified Fowler–Nordheim expression may be applicable for tunnelling through the interfacial barrier when the electric field at the barrier was sufficiently high to reduce the barrier width to about 5 nm. Therefore the data in this region were replotted as a Fowler–Nordheim plot ( $\log(I/V^2)$  versus  $1/V$ ) following Eq. (18) and yielded a straight line with negative slope. From Eq. (18), the slope of such a plot is  $-6.83 \times 10^9 d_i \phi^{3/2} \text{ V}^{-1}$  where the barrier thickness  $d_i$  is in metres and the barrier height  $\phi$  is in electronvolts. Assuming a typical value of the tunnelling thickness of  $d_i = 5 \text{ nm}$ , barrier heights of 0.36 eV and 0.27 eV were derived respectively for an In|CuPc|In sample and a similar sample incorporating an insulating “edge-thickening” layer to avoid localized dielectric breakdown. Although this analysis confirmed that a conductivity relationship of the Fowler–Nordheim type was followed, it was also pointed out that the value of the current density predicted by this expression was considerably higher than that actually observed. This reduction in the observed current density below the theoretical value was consistent with an effective tunnelling area considerably less than the geometric area. According to

Chopra [93], a factor as low as  $10^{-5}$  may be applicable. Another contributing factor to the current density reduction is undoubtedly the effect of traps in the CuPc film; Geppert [94] has shown that in the presence of traps current density may also be reduced below the Fowler–Nordheim value. Therefore it was proposed [72] that a modified tunnelling process took place at the bottom injecting electrode, and that the current density was reduced by a combination of the two effects described above.

A more rigorous test for tunnelling behaviour in phthalocyanine films would be to perform measurements on sandwich structures with a phthalocyanine film thickness of less than 10 nm. However, in view of the relatively large size of the phthalocyanine molecule compared with the film thickness, the growth of high-quality films of this material using conventional techniques is unlikely. Measurements on Langmuir–Blodgett films, where the film thickness and quality can be more precisely controlled, offer a possibility, although the difficulties in the application of evaporated contacts to such films should not be underestimated.

### 3.6. The Schottky effect

Field-assisted lowering of the potential barrier at a blocking contact in phthalocyanine thin films has been observed in several materials, often in Schottky diode devices under reverse bias. Füstös–Wegner [95] investigated the electrical properties of  $\alpha$ -form  $H_2Pc$  films supplied with Al and Au electrodes, finding the familiar linear  $\log J$  versus  $V^{1/2}$  dependence when both electrodes were Al. This was ascribed to either Schottky emission from the electrodes or Poole–Frenkel emission. Similarly, Barkhalov and Vidadi [96] observed this type of behaviour for the reverse-bias direction of Al|CuPc|Ag structures. Hamann and Tantzsch [41] studied CuPc films supplied either with two Al electrodes or with one Al and one Au electrode. It was proposed that an aluminium oxide layer grew at the interface with the Al electrode, probably by diffusion of oxygen from the organic material. The devices were envisaged as a series combination of Schottky emission over the oxide layer and SCLC over the CuPc layer. The Schottky effect was negligible for CuPc film thicknesses greater than 1.5  $\mu m$ . A similar explanation was also advanced by Fan and Faulkner [97] to explain their measurements on CuPc and ZnPc films. A barrier height of 1.27 eV was determined in ZnPc films with Al electrodes. The Schottky barrier width in such samples was estimated to be approximately 6.5 nm, which is similar to the reported thickness of naturally grown  $Al_2O_3$  films at room temperature.

Tripathi et al. [98] observed the Schottky effect in CuPc pellets using tin electrodes, and found a barrier height of 0.37 eV and a  $\beta_s$  value consistent with a relative permittivity of 3.2, as obtained from ac measurements. Wilson and Collins [12] obtained a linear dependence of the logarithm of current on  $V^{1/2}$  as predicted by Eq. (22) for planar films of CuPc with Al electrodes. By comparison of the measured slope of their plot with that expected for a material with relative permittivity  $\epsilon_r = 3.8$ , a depletion region width of 96 nm was derived which was comparable to that derived by Vidadi et al. [99]. However, a similar calculation applied to their measurements with silver electrodes yielded an unreasonable depletion region width

of 240 nm, suggesting that in this case the simple Schottky effect was not solely responsible for the observed behaviour.

Hassan and Gould [63] observed a linear dependence of  $\log J$  on  $V^{1/2}$  in CuPc films with a positively biased Al electrode. The theoretical value of  $\beta_s = 2 \times 10^{-5} \text{ eV m}^{1/2} \text{ V}^{-1/2}$  from Eq. (20) was considerably lower than the calculated value of  $\beta = 9.4 \times 10^{-5} \text{ eV m}^{1/2} \text{ V}^{-1/2}$  for an oxygen-doped sample and  $\beta = 13.2 \times 10^{-5} \text{ eV m}^{1/2} \text{ V}^{-1/2}$  for an annealed sample, both for voltages less than about 16 V. (For higher voltages the measured  $\beta$  values were lower, and consistent with the Poole–Frenkel effect described in Section 3.3.) The  $\beta$  values derived from the lower-voltage sections of the curves were thus a factor of 4.7 (oxygen-doped) or 6.6 (annealed) times the theoretical Schottky values, sufficiently at variance to eliminate an interpretation based on the effect occurring across the entire CuPc thickness of 5  $\mu\text{m}$ . However, following the conclusions of Wilson and Collins [12] that most of the applied voltage is dropped across a depletion region of thickness  $d_s$  and assuming the theoretical value of  $\beta_s$ , the values of  $d_s$  and the Schottky barrier height  $\phi_0$  were determined using Eq. (23). The data yielded values of  $d_s = 220 \text{ nm}$  and  $\phi_0 = 1 \text{ eV}$  for the oxygen-doped sample, and  $d_s = 120 \text{ nm}$  and  $\phi_0 = 0.88 \text{ eV}$  for the annealed sample. These values of  $d_s$  are reasonably consistent with those of Wilson and Collins, and therefore it appeared that annealing reduced both the depletion region thickness and the barrier height. For Au/CuPc/Pb samples [74] in the lower voltage range, values of  $\beta$  7.0 times and 4.4 times the theoretical  $\beta_s$  value were derived for the injecting Pb electrode on the substrate and on the non-substrate side respectively of the CuPc films. A similar analysis based on the existence of a Schottky barrier at the injecting electrode yielded  $d_s = 40 \text{ nm}$  and  $\phi_0 = 1 \text{ eV}$  for the Pb electrode on the substrate side, and  $d_s = 100 \text{ nm}$  and  $\phi_0 = 1 \text{ eV}$  for the Pb electrode on the non-substrate side. Thus on the non-substrate side of the CuPc the Pb electrode formed a wider depletion region than on the substrate side, probably due to either surface roughness effects as observed in  $\text{H}_2\text{Pc}$  layers [100] or a transition from the  $\alpha$  to the  $\beta$  phase owing to the elevated temperatures experienced during electrode deposition.

In oxygen-doped triclinic PbPc films with an Al top electrode and a Au bottom electrode Ahmad and Collins [87] used a Schottky barrier analysis to interpret results for injection from the Al electrode. Values of  $d_s = 50 \text{ nm}$  and  $\phi_0 = 1.11 \text{ eV}$  for voltages up to about 2 V and  $d_s = 488 \text{ nm}$  and  $\phi_0 = 1.036 \text{ eV}$  for higher voltages were obtained. Measurements by these workers on samples with a bottom Al electrode and a top Au electrode showed similar behaviour, but with a narrower depletion width in each voltage range. Shafai and Gould [13,76] found  $d_s = 50 \text{ nm}$  and  $\phi_0 = 1 \text{ eV}$  for similar samples with an Al top electrode at voltages up to about 4 V, in excellent agreement with the results obtained by Ahmad and Collins in a similar voltage range.

Therefore there appears to be a general body of evidence that a linear  $\log J$  versus  $V^{1/2}$  dependence is observed for hole injection at blocking contacts into various phthalocyanine thin films. A discrete change in the  $\beta$  value has been observed in CuPc films with an injecting Al electrode [63], CuPc films with a Pb electrode [74] and PbPc films with an Al electrode [13,76,87]. Derived  $\beta$  values are normally in excess of the theoretical  $\beta_s$  value at low voltages, and thus there is general agreement

on interpretations based on Schottky emission over a narrower depletion region at the injecting electrode. At higher voltages both an increase in the Schottky barrier width and the establishment of Poole–Frenkel or modified Poole–Frenkel conductivity have been proposed.

### 3.7. Diode-type conductivity

The diode equation (24) is followed under forward-bias conditions when a metal semiconductor junction controls the overall conductivity. Fan and Faulkner [97] observed such behaviour in  $\text{In}|\text{H}_2\text{Pc}|\text{Au}$  and  $\text{In}|\text{ZnPc}|\text{Au}$  structures. For the former structure the diode equation was followed below a voltage of about 0.3 V and the analysis yielded a barrier height  $\phi_b$  in Eq. (25) of 1.5 eV. This value accorded reasonably well with an estimate based on the ionization potential of  $\text{H}_2\text{Pc}$  and the work function of In. For the latter structure, similar behaviour was observed with  $\phi_b = 1.35$  eV and the diode quality factor  $\eta = 1.37$ . Loutfy et al. [101] investigated the barrier between In and  $\text{H}_2\text{Pc}$  during their work on phthalocyanine organic solar cells. These workers also observed exponentially increasing values of  $J$  with  $V$  at applied voltages below 0.5 V, which were accounted for in terms of a modified Shockley equation involving the device series and shunt resistances. Values of the diode quality factor  $\eta = 1.3$ –2.6 were derived from these results. Capacitance measurements yielded values of  $\phi_b = 0.63$  eV and Schottky barrier width 29 nm. Martin et al. [102] measured the junction properties in  $\text{Au}|\text{ZnPc}|\text{metal}$  (where the metal was Au, Cu, Cr, Al, In, or Sm) both in a vacuum and after exposure to air. Similarly, they found diode-type behaviour with a rectification ratio RR (defined as the ratio of the currents under forward and reverse bias at a voltage of  $\pm 0.5$  V) having a particularly high value of 82 for an Al electrode after exposure to air. Therefore the strong rectification effect was correlated with the presence of oxygen.

Hamann et al. [103] noticed diode behaviour in thin-film  $\text{Ni}|\text{PbPc}$  junctions for voltages up to 0.2 V, provided that the deposition was performed at room temperature. This type of conduction was believed to result from weak oxidation of the Ni contact. Conversely, samples deposited at higher temperatures, where the crystallite size was larger and the barrier height lower, showed SCLC. Abdel-Malik et al. [104] reported diode-type characteristics in films of  $\beta$ -phase  $\text{CoPc}$  dispersed in a polymer binder, from which a value of  $\eta = 2.45$  was determined. In this work a modified Shockley equation, identical with that previously used by Loutfy et al. [101], was adopted. Shimura and Toyoda [105] made measurements on fluoroaluminium phthalocyanine ( $\text{AlPcF}$ ) films, studying their photovoltaic properties. They used a  $\text{Sn}|\text{AlPcF}|\text{Au}$  structure which showed rectifying diode-type behaviour described by Eq. (24), with  $\eta = 1.45$  and an RR value of about 33 measured at  $\pm 1$  V.

Measurements on  $\text{CuPc}$  films with combinations of Au and Pb electrodes were reported by Gould and Hassan [74]. Both  $\text{Pb}|\text{CuPc}|\text{Au}$  and  $\text{Au}|\text{CuPc}|\text{Pb}$  samples (where the first metal is adjacent to the substrate) showed current densities lower than in  $\text{Au}|\text{CuPc}|\text{Au}$  samples. Moreover, reverse-bias current densities were considerably lower than those for forward bias. In both these respects the characteristics resembled those of  $\text{Au}|\text{CuPc}|\text{Al}$  samples where a Schottky barrier was shown to

exist at the Al contact [12,63]. For Pb|CuPc|Au samples under a forward bias of less than 1 V, a linear dependence of  $\ln J$  on  $V$  was obtained, showing similar behaviour to that found by Loutfy et al. [101] in  $H_2$ Pc with In electrodes. There was good correlation with Eqs. (24) and (25), and values of  $\eta = 1.6$  and  $\phi_0 = 1.05$  eV were obtained. A high RR value of 790 (measured at  $\pm 1$  V) was found for this type of sample. However, typical diode behaviour following Eq. (24) was not observed in Au|CuPc|Pb samples. Furthermore, both the forward and the reverse current densities for samples of this configuration were lower than for Pb|CuPc|Au samples, with an RR value of only 7 for a freshly prepared sample. Since in this type of sample the Pb|CuPc interface is on the non-substrate side of the CuPc film, a controlling potential barrier or interface region might be expected, one effect of which is to lower RR. After annealing at approximately 150 °C and subsequent exposure to air for 5 h, an increase in the value of RR to 74 was observed. This effect had previously been reported by Martin et al. [102], in particular in Au|ZnPc|Al samples where RR increased from a value of 1 to 82. This was attributed to the development of an enhanced space-charge region within the ZnPc, a process which would also satisfactorily explain the later results in CuPc using Pb electrodes.

Ahmad and Collins [87] observed diode-type conductivity in Au|PbPc|Al devices. They found a linear dependence of  $\ln J$  on  $V$  with values of  $\eta = 1.9$  and  $\phi_0 = 1.108$  eV using the analysis of Eqs. (24) and (25). These attributes were also extracted from the data using the more sophisticated method of Cheung and Cheung [106], which also takes into account the diode series resistance  $R$  and which is appropriate for non-ideal diodes ( $\eta \neq 1$ ). The results of this analysis were  $\eta = 1.7$ ,  $\phi_0 = 1.126$  eV and  $R = 530$  M $\Omega$ , which are in good agreement with the values obtained by the simpler method. A value of RR of 40 at  $\pm 1$  V was also determined. For Al|PbPc|Au devices (Al adjacent to the substrate) they found  $\eta = 2.09$ ,  $\phi_0 = 1.144$  eV and an RR value of 8. Therefore the latter parameter was higher when the Al contact was on the non-substrate side of the films.

Despite the apparent similarities between the results of work performed on films of CuPc [74] and PbPc [87], there are significant differences in both the methods of preparation and the detailed results. The CuPc film structures were prepared in a single deposition sequence without breaking vacuum so that incorporation of oxygen into the films was minimized. In this work diode behaviour was only observed when the Pb electrode was on the substrate side of the films and showed a very high value of RR. Conversely, the PbPc films were deposited in a different vacuum system to that used for the bottom electrode, during which an  $Al_2O_3$  layer could form if the bottom electrode were Al. Additionally, the samples were exposed to dry air for a period of several weeks before deposition of the top electrode. Diode behaviour occurred irrespective of the electrode positions, but in this case the highest RR values occurred when the Al electrode was on the non-substrate side, although its value was considerably lower than that for the CuPc samples. However, both sets of workers were in agreement that the development of an interfacial layer, resulting from the effect of oxygen exposure, was a controlling factor in device operation and that asymmetric conduction behaviour was related to this. More recently, Kašpar et al. [88] have re-examined potential barrier formation caused by absorption of

negatively charged oxygen molecules on the PbPc surface, and stressed the importance of a reported increase in barrier height and a decrease in barrier width due to annealing. It was suggested that a slow release of absorbed oxygen under vacuum, enhanced at higher temperatures, was responsible for these effects. Clearly, additional work on different types of phthalocyanine films, supplied with various combinations of electrode materials, is required before the diode-type conduction behaviour is fully understood.

#### 4. Ac electrical properties

The ac properties in phthalocyanine thin films have been studied considerably less than the dc properties. Because of this general paucity of data it is worthwhile briefly reviewing some ac measurements on bulk samples. Bradley et al. [107] studied the ac properties of powdered  $\beta$ -form  $H_2Pc$  compressed at pressures above 10 kbar; for dc work, measurements made under these conditions were considered to yield true conductivity values. The intergranular capacitance for high frequency ac provided a low-impedance shunt across the contact resistance, and an equivalent resistance and capacitance network was proposed to account for the conduction behaviour. In general, the resistance was found to decrease with increasing frequency, or the conductivity increased with increasing frequency. Fendley and Jonscher [108] made similar measurements of conductivity and capacitance on compressed CuPc crystallites over a wide frequency range of  $10^2$ – $10^{10}$  Hz, using a wide variety of measuring techniques appropriate to the various frequency ranges. The major fact to emerge from this work was that the conductivity  $\sigma$  followed a power-law dependence on the angular frequency  $\omega$ , or  $\sigma \propto \omega^n$  with  $n = 0.8$ . These workers pointed out the great similarity of this behaviour to that observed in a wide range of materials in which hopping was believed to occur. Thus, although the possibility of hopping in phthalocyanine materials was inferred from ac measurements by 1972, identification of hopping in thin films using dc methods is a much more recent event [52,64]. Sadaoka and Sakai [109] also concluded that hopping was a major conduction process in CuPc, observing  $\sigma \propto \omega^n$  not only for compressed powders but also for thin films. Similarly Wacławek et al. [110] observed both hopping and thermally activated behaviour in CuPc, CoPc and PbPc compressed powders and films. Nalwa and Vasudevan measured dielectric properties of pellets of both CoPc [111] and chloro-iron phthalocyanine [112]. CoPc showed an increase in  $\epsilon_r$  with temperature up to approximately 150 °C, above which a sharp decrease took place. A similar dependence was displayed for the loss tangent  $\tan \delta$ . This behaviour was associated with nomadic polarization effects. In chloro-iron phthalocyanine the values of both  $\epsilon_r$  and  $\tan \delta$  increased with temperature in the range 20–260 °C (293–533 K), showing higher values at 1 kHz than at 10 kHz. Nomadic polarization was also considered to be responsible for this behaviour. Abdel-Malik et al. [113] measured ac properties in  $H_2Pc$ , NiPc and CuPc pellets, and also observed the  $\sigma \propto \omega^n$  law. Measurements were made for 303–513 K and 10– $10^5$  Hz. Measurements of conductivity as a function of reciprocal temperature showed very little variation except at high temperatures.

In the higher-temperature range the conductivity remained essentially constant over the whole frequency range. Identical conclusions were made to those drawn for CuPc and magnesium phthalocyanine (MgPc) films in the earlier work of Vidadi et al. [114] which is described below. Thus there is reasonable evidence that bulk phthalocyanines exhibit hopping effects, particularly at low temperatures, with several materials showing a  $\sigma \propto \omega^n$  dependence [108–110,113], and an equivalent circuit model has been proposed to account for variations in conductivity as a function of frequency [107]. These results are closely related to the ac measurements on thin films described below.

Vidadi et al. [114] pointed out that both hopping and band-type mechanisms may be operative in organic materials, with the predominance of either depending on the conditions of temperature and frequency. They fabricated sandwich structures of CuPc and MgPc using unspecified metallic electrodes. A general increase in conductivity with frequency was observed, consistent with the carriers possessing a wide range of relaxation times. Conductivity was also strongly temperature dependent, although the frequency dependence was less pronounced at higher temperatures. Thus it was concluded that the charge carrier transport was of the free-band type in the high-temperature low-frequency region, and was mainly by hopping in the low-temperature high-frequency region. A value of  $n = 1.75$  for the  $\sigma$ - $\omega$  power-law exponent was quoted for CuPc films at frequencies of  $10^4$ – $10^6$  Hz. Other early measurements on CuPc films were performed during work on bulk samples and similarly showed the usual  $\sigma \propto \omega^n$  dependence [109]. Values of  $n < 1$  were determined by Wacławek et al. [110] for CuPc, CoPc and PbPc films.

A comprehensive series of measurements were made by Vidadi et al. [115] on CuPc films supplied with two blocking electrodes of Al. Capacitance and loss tangent were measured as functions of temperature and frequency. Since the electrodes were blocking, they had a considerable influence on the ac conductivity of the structures, and it was proposed that the equivalent circuit model of Simmons et al. [116] was applicable to these results. In this model the Schottky barriers are represented by the Schottky capacitance  $C_s$  and the interior of the structure by a capacitance  $C_b$  shunted by a thermally activated resistance  $R_b = R_0 \exp(\phi/kT)$ , where  $\phi$  represents an activation energy. The various frequency and temperature dependences are fully explained in Ref. [116]. The equivalent circuit representation is shown in Fig. 7(a). Several important features observed by Vidadi et al. were (i) a strong increase in capacitance with increasing temperature, (ii) a decrease in capacitance with increasing frequency, with greater changes taking place at higher temperatures, and (iii) a maximum in the  $\tan \delta$ -frequency characteristic which shifted to higher frequencies with increasing temperature. These were all in accordance with the model. The Schottky barrier width was determined as  $0.1 \mu\text{m}$  and the total trap concentration in the CuPc films as  $3 \times 10^{22} \text{ m}^{-3}$ . A comparable dependence of capacitance on frequency as a function of temperature was exhibited by Al[CuPc]Ag samples [96]. The dependence of Schottky barrier capacitance in MgPc [117] and ZnPc [83] as a function of frequency has been investigated. Again, there was a large increase in capacitance with increasing temperature and a decrease with increasing frequency.

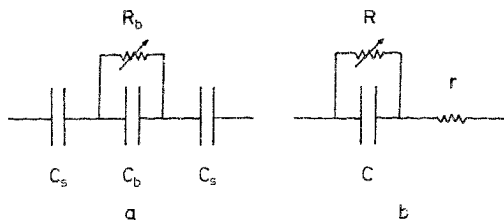


Fig. 7. Simple equivalent circuit models employed in the analysis of the ac properties of phthalocyanine thin-film sandwich structures. These models have been applied to films with (a) two blocking contacts (Schottky barriers) and (b) two ohmic contacts. After Refs. [116] and [123] respectively.

However, the frequencies used in this work were very low: 0.1–100 Hz for MgPc and  $10^{-2}$ –1 Hz in ZnPc.

Boudjema et al. [34] also made extensive measurements of conductance, capacitance and loss tangent as functions of frequency in the range  $10^{-3}$ – $10^5$  Hz in NiPc and ZnPc films. The samples had one Au electrode and the other was of Al, In or Au, and the temperatures were not varied. For a Au|NiPc|Au sample conductance increased with increasing frequency,  $\tan \delta$  decreased and capacitance decreased. Conversely, for a Au|ZnPc|In sample the conductance reached a plateau at high frequencies whose value was determined by the electrical properties of the bulk, and at lower frequencies a similar plateau was observed whose conductance value depended on a space-charge region at an electrode interface. The capacitance increased by nearly two orders of magnitude in the very low-frequency region, and a broad maximum was observed in  $\tan \delta$  at approximately  $10^2$  Hz. Furthermore, measurements performed with various applied dc voltages showed a complex series of results. These workers concluded that samples with two Au electrodes behaved as expected for ohmic contacts, whereas the other samples generally behaved as if at least one Schottky barrier was present. The space-charge region in the latter case extended into the phthalocyanine and was related to oxygen absorption. A three-layer equivalent circuit model, consisting of circuit elements to model a surface charge layer, a space-charge layer and a bulk layer, was presented. The various measured parameters were found to be in general agreement with the predictions of this model. However, the model is rather complex and, as has been shown above, the ac measurements of Vidadi et al. [115] were satisfactorily explained in terms of the model of Simmons et al. [116], although the frequency range concerned was considerably less than that applied by Boudjema et al. [34]. In addition, measurements of similar type were also reported by Maitrot et al. [118] for phthalocyanine films doped during deposition by cosublimation. More recently, Abdel-Malik [119] made simple measurements of capacitance as a function of temperature in structures consisting of FePc dispersed in a polymer binder and having one Al and one Au electrode. Measurements were performed at frequencies of 8 and 25 kHz. In accordance with ac electrical measurements on other phthalocyanine films, capacitance



increased with increasing temperature and decreased with increasing frequency, and was associated with the slow release of charge carriers from relatively deep traps.

James et al. [89] measured the dielectric and optical properties of molybdenum phthalocyanine (MoPc) films in the frequency range 10 kHz–1 MHz. The films were deposited on conducting indium tin oxide (ITO) glass substrates and the sandwich structures were completed using Cu electrodes. The conductance increased and the capacitance decreased with increasing frequency, and there was a linear dependence of the logarithm of conductivity on the logarithm of frequency, implying the usual  $\sigma \propto \omega^n$  dependence, which was interpreted in terms of hopping conduction. A maximum in  $\tan \delta$ , as predicted by the model of Simmons et al. [116], was observed at 190 kHz and was associated with a room temperature relaxation time of 798  $\mu$ s. A Debye relaxation time of 878  $\mu$ s was also estimated, together with an average relaxation time of 942  $\mu$ s using the Cole–Cole model. Following this, Gould and Hassan [90] measured ac conductivity  $\sigma(\omega)$ , capacitance and  $\tan \delta$  in CuPc films with ohmic Au electrodes for the frequency range  $10^2$ – $2 \times 10^4$  Hz and for temperatures from 173 to 360 K.  $\sigma(\omega)$  increased with temperature and with frequency, and the power-law exponent also tended to increase with increasing frequency and decrease with increasing temperature. This type of behaviour was associated with a hopping process at low temperatures and high frequencies. It was suggested that the conductivity might follow the expression derived by Elliott [120]

$$\sigma(\omega) = \frac{\pi^2 N^2 \epsilon_r \epsilon_0}{24} \left( \frac{8e^2}{\epsilon_r \epsilon_0 W_m} \right)^6 \frac{\omega^s}{\tau_0^\beta} \quad (26)$$

where  $N$  represents the density of localized states,  $\epsilon_r \epsilon_0$  is the permittivity,  $e$  is the electronic charge and  $\tau_0$  is the effective relaxation time (approximately  $10^{-13}$  s). The power-law exponent  $s$  in this model is given by  $1 - \beta$  at low temperatures where  $\beta = 6kT/W_m$  and  $W_m$  is the optical energy gap. Reasonable agreement with this expression for correlated barrier hopping was observed with  $s$  tending to unity at low temperatures and high frequencies. The question is left open as to whether other types of hopping conduction may eventually offer a more appropriate description of ac conductivity in phthalocyanine thin films. Various different variations of  $s$  with frequency and temperature are described in the literature [121,122] which may in due course prove to offer a better fit to the data over a wider range of frequency. The dependence of  $\sigma(\omega)$  on  $1/T$  showed a region of free-band conductivity, with activation energy 0.3 eV, at higher temperatures and very low activation energies, associated with hopping, at lower temperatures. Capacitance decreased with increasing frequency and increased with increasing temperature. However,  $\tan \delta$  decreased with increasing frequency and was consistent with the appearance of a minimum at a higher frequency. This contrasts with the  $\tan \delta$  behaviour in CuPc films with blocking Al electrodes as described by Vidadi et al. [115] in which a maximum occurred. The difference between the two sets of results appears to result from the application of ohmic contacts in the former case, for which the equivalent circuit model of Simmons et al. [116] is inappropriate. Therefore an alternative equivalent circuit model, suggested by Goswami and Goswami [123], was adopted; this model

was originally proposed for ZnS films sandwiched between Al electrodes, which act as ohmic contacts for n-type materials. In this model the system is assumed to comprise a frequency-independent capacitive element  $C$  in parallel with a discrete temperature-dependent resistive element  $R$ , both in series with a low-value resistance  $r$  which represents the leads and contacts. The equivalent circuit for this model is shown in Fig. 7(b).  $R$  is assumed to be thermally activated and to follow the same law as in the model of Simmons et al. However, the Schottky barrier capacitance is absent, and the differences between the predictions of the two models result from this. Equations for the dependences of capacitance and  $\tan \delta$  derived from this model are consistent with the behaviour observed. Moreover, a decrease in both conductance and capacitance after annealing is also compatible with an increase in the value of  $R$  owing to the desorption of oxygen which acts as an acceptor impurity.

These results have subsequently been confirmed in both ZnPc films [91] and CoPc films [92] supplied with ohmic Au electrodes. In the former case there was a decrease in conductivity above about 426 K which was identified with the  $\alpha$  to  $\beta$  phase transition and the desorption of oxygen. The free-band activation energy was 0.29 eV in ZnPc and the rather higher value of 0.54 eV in CoPc. A decrease in both the conductance and the capacitance after annealing was found in both these materials.

Thus in general ac measurements show  $\sigma \propto \omega^n$  behaviour, indicative of hopping. At higher temperatures and lower frequencies free-band conduction is often observed. Capacitance and  $\tan \delta$  variations in many films show behaviour which has been explained using equivalent circuit models for blocking contacts [116] or ohmic contacts [123], or require a more complex three-layer model [34]. A more complete correlation between experiment and theoretical predictions must await the development of hopping and equivalent circuit models specifically for organic semiconductor films and their associated contacts.

## 5. Summary and conclusions

In this review the present state of knowledge of the structure and electrical conduction properties of evaporated phthalocyanine thin films has been examined. Structural considerations are important in conductivity measurements in that the intrinsic conductivity of the various structural forms differ, and the  $\alpha$  form appears to exhibit a higher propensity to absorb oxygen than the  $\beta$  form. It is fairly well established that the  $\beta$  form of most phthalocyanines has the monoclinic structure, while the  $\alpha$  form has been variously reported as tetragonal, orthorhombic and, more recently, monoclinic. Films deposited at room temperature are usually of the metastable  $\alpha$  phase, but they undergo a phase transformation to the stable  $\beta$  phase on annealing. Recent work on CuPc and CoPc has confirmed that the  $\alpha$ -form films are preferentially orientated but become more randomly orientated with increasing thickness. The  $\alpha$  to  $\beta$  phase transformation in CoPc films has been directly observed by X-ray diffraction methods. Because of the relatively large size of the central metal atom, the atypical PbPc molecule is shaped like a shuttlecock. This results in the

existence of two major structures, the low-temperature monoclinic phase and the high-temperature triclinic phase. These two phases have recently been observed in thin films deposited onto substrates maintained at 323 and 533 K respectively.

Several dc conduction mechanisms have been identified in phthalocyanine thin films depending on the type of electrodes provided, the voltage range, the temperature and the thickness. Most phthalocyanine films, when deposited in the form of a sandwich structure and equipped with at least one ohmic electrode (usually Au), exhibit space-charge-limited conductivity. In many cases this is controlled by an exponential distribution of traps, although discrete trap levels have also been observed, usually after exposure to oxygen. There are reports of Poole–Frenkel emission above a voltage of approximately 2–4 V in CuPc and PbPc films, where the injecting electrode also shows Schottky barrier field-lowering at lower voltages. In some cases the measured Poole–Frenkel coefficient is larger than the theoretical value, indicative of enhanced electric fields within the phthalocyanine films. Hopping conductivity under dc conditions, corresponding to the Mott  $T^{-1.4}$  law, has been reported in (FePc)K and in PbPc films, although it is curious that dc hopping has not been observed more frequently, particularly in view of its role in ac conductivity. Fowler–Nordheim tunnelling has been identified in CuPc films with In electrodes, for which it was proposed that an interfacial oxide layer was responsible for modifying the character of the In|CuPc contact, thus allowing tunnelling to occur. In samples with at least one blocking contact, field-lowering of a Schottky potential barrier has been reported in the reverse-bias direction. In the forward direction conventional Schottky-diode-type behaviour has been observed. Measured  $\beta$  values are often in excess of the theoretical value for the Schottky effect, and interpretations based on Schottky emission over a narrow depletion region thickness are common. Such behaviour has been reported mainly in CuPc with either an Al or a Pb electrode, and in PbPc with an Al electrode. Schottky barriers with typical widths and barrier heights of 200 nm and 1 eV respectively were observed in these structures. Under forward bias, diode behaviour has been identified for several electrode–phthalocyanine combinations, yielding comparable values for the barrier height to those derived under reverse-bias conditions. Diode quality factors in the range 1.3–2.45 were measured, and rectification ratios of up to 790 have been reported.

Ac measurements have generally shown a  $\sigma \propto \omega^n$  dependence for low temperatures and high frequencies, corresponding to hopping conduction. At higher temperatures and lower frequencies free-band conductivity with an activation energy of a few tenths of an electronvolt is fairly common. Capacitance and loss tangent variations with both frequency and temperature have been accounted for using various equivalent circuit models applicable to ohmic and blocking electrodes. Thermal activation of carriers in the interior of the phthalocyanine films is frequently assumed.

In conclusion, it should be stressed that, although phthalocyanine thin films have been extensively investigated, as yet an overall consensus view of the relative importance of their various features has not been achieved. It is clear that phthalocyanines are considerably less pure than inorganic semiconductors, even after entrained sublimation, and therefore that impurities and traps are likely to be a dominant feature in determining the conductivity. Furthermore, owing to the propensity of phthalocya-

nines to absorb oxygen and other gases, it would appear that annealing is always necessary before measurements of the intrinsic properties are attempted. It is possible that significant further progress will require improved deposition processes such as organic molecular beam epitaxy or the Langmuir-Blodgett technique. The use of a zero-gravity growth environment has already been explored, and may become routine in the future. Owing to the methods of synthesis of phthalocyanines, it is unlikely that the purity can be significantly improved by further developments of present techniques. Improved materials deposition and characterization is probably the key to further advances in both the structural and the electronic fields.

### Acknowledgements

Thanks are due to my former and present research students Torfeh Shafai, Qun Zhou and Dr. Ascel Hassan, especially the latter whose thesis has been plundered in the search for reference material. Salah Shihub has also helped in the provision of references and has critically read the work in draft form, a task also carried out by Dr. Salvatore Gravano. The author is very grateful for their comments, and confirms that any remaining errors are entirely his own responsibility.

### References

- [1] F.H. Moser and A.L. Thomas, *The Phthalocyanines*. CRC Press, Boca Raton, FL, 1983.
- [2] R.P. Linstead, *J. Chem. Soc.*, (1934) 1016.
- [3] C.E. Dent, R.P. Linstead and A.R. Lowe, *J. Chem. Soc.*, (1934) 1033.
- [4] D.D. Eley, *Nature (London)*, 162 (1948) 819.
- [5] A.T. Vartanyan, *Zh. Fiz. Khim.*, 22 (1948) 769.
- [6] G.H. Heilmeyer and G. Warfield, *J. Chem. Phys.*, 38 (1963) 163.
- [7] A. Rose, *Phys. Rev.*, 97 (1955) 1538.
- [8] G.H. Heilmeyer and S.E. Harrison, *Phys. Rev.*, 132 (1963) 2010.
- [9] A. Sussman, *J. Appl. Phys.*, 38 (1967) 2738.
- [10] A. Sussman, *J. Appl. Phys.*, 38 (1967) 2748.
- [11] C. Hamann, *Phys. Status Solidi*, 26 (1968) 311.
- [12] A. Wilson and R.A. Collins, *Sensors and Actuators*, 12 (1987) 389.
- [13] T.S. Shafai and R.D. Gould, *Int. J. Electron.*, 73 (1992) 307.
- [14] K. Ukei, *Acta Crystallogr.* B29 (1973) 2290.
- [15] Y. Iyechika, K. Yakushi, I. Ikemoto and H. Kuroda, *Acta Crystallogr.* B38 (1982) 766.
- [16] P.M. Burr, P.D. Jeffery, J.D. Benjamin and M.J. Uren, *Thin Solid Films*, 151 (1987) L111.
- [17] R.A. Collins, M.K. Ellis and T.A. Jones, *Chemtronics*, 5 (1991) 93.
- [18] J.D. Wright, *Prog. Surf. Sci.*, 31 (1989) 1.
- [19] K. Wilksne and A.E. Newkirk, *J. Chem. Phys.*, 34 (1961) 2184.
- [20] J.M. Robertson, *J. Chem. Soc.*, (1935) 615.
- [21] A.A. Ebert and H.B. Gottlieb, *J. Am. Chem. Soc.*, 74 (1952) 2806.
- [22] F.W. Karasek and J.C. Decius, *J. Am. Chem. Soc.*, 74 (1952) 4716.
- [23] M.T. Robinson and G.E. Klein, *J. Am. Chem. Soc.*, 74 (1952) 6294.
- [24] J.M. Assour, *J. Phys. Chem.*, 69 (1965) 2295.
- [25] M. Ashida, N. Uyeda and E. Suito, *Bull. Chem. Soc. Jpn.*, 39 (1966) 2616.
- [26] M. Ashida, N. Uyeda and E. Suito, *J. Cryst. Growth*, 8 (1971) 45.

- [27] C.J. Brown, J. Chem. Soc. A, (1968) 2488.
- [28] C.J. Brown, J. Chem. Soc. A, (1968) 2494.
- [29] K.F. Schoch, J. Gregg and T.A. Temofonte, J. Vac. Sci. Technol. A, 6 (1988) 155.
- [30] J.H. Sharp and A. Abkowitz, J. Phys. Chem., 77 (1973) 477.
- [31] J.M. Assour and W.K. Kahn, J. Am. Chem. Soc., 87 (1965) 207.
- [32] F. Iwatsu, T. Kobayashi and N. Uyeda, J. Phys. Chem., 84 (1980) 3223.
- [33] M.S. Mindorff and D.E. Brodie, Can. J. Phys., 59 (1981) 249.
- [34] B. Boudjema, G. Guillard, M. Gamoudi, M. Maitrot, J.-J. André, M. Martin and J. Simon, J. Appl. Phys., 56 (1984) 2323.
- [35] M. Komiyama, Y. Sakakibara and H. Hirai, Thin Solid Films, 151 (1987) L109.
- [36] G.A. Williams, B.N. Figgis, R. Mason, S.A. Mason and P.E. Fielding, J. Chem. Soc. Dalton Trans., (1980) 1688.
- [37] B.N. Figgis, E.S. Kucharski and P.A. Reynolds, J. Am. Chem. Soc., 111 (1989) 1683.
- [38] M.K. Debe and K. K. Kam, Thin Solid Films, 186 (1990) 289.
- [39] A.K. Hassan and R.D. Gould, Phys. Status Solidi A, 132 (1992) 91.
- [40] C. Hamann and H. Wagner, Krist. Tech., 6 (1971) 307.
- [41] C. Hamann and C. Tantzsch, Thin Solid Films, 36 (1976) 81.
- [42] S.I. Shihub and R.D. Gould, Phys. Status Solidi A, 139 (1993) 129.
- [43] K.A. Mohammed and R.A. Collins, Thermochim. Acta, 104 (1984) 277.
- [44] J.H. Sharp and R.L. Miller, J. Phys. Chem., 72 (1968) 3335.
- [45] E.A. Lucia and F.D. Verderame, J. Chem. Phys., 48 (1968) 2674.
- [46] J.R. Fryer, Acta Crystallogr., A35 (1979) 327.
- [47] R.A. Collins, A. Krier and A.K. Abass, Thin Solid Films, 229 (1993) 113.
- [48] R.A. Collins and A. Belgachi, Mater. Lett., 9 (1989) 349.
- [49] K. Ukei, K. Takamoto and E. Kanda, Phys. Lett. A, 45 (1973) 345.
- [50] H. Yasunaga, K. Kojima, H. Yohda and K. Takeya, J. Phys. Soc. Jpn., 37 (1974) 1024.
- [51] F. Gutmann and L.R. Lyons, Organic Semiconductors, Wiley, New York, 1967.
- [52] A. Ahmad and R.A. Collins, Thin Solid Films, 217 (1992) 75.
- [53] J.G. Simmons, J. Phys. D, 4 (1971) 613.
- [54] D.R. Lamb, Electrical Conduction Mechanisms in Thin Insulating Films, Methuen, London, 1967.
- [55] M.A. Lampert, Rep. Prog. Phys., 27 (1964) 329.
- [56] R.D. Gould and M.S. Rahman, J. Phys. D, 14 (1981) 79.
- [57] R.D. Gould and B.A. Carter, J. Phys. D, 16 (1983) L201.
- [58] R.D. Gould, J. Appl. Phys., 53 (1982) 3353.
- [59] R.D. Gould, J. Phys. D, 9 (1986) 1785.
- [60] A. Ahmad and R.A. Collins, Phys. Status Solidi A, 123 (1991) 201.
- [61] M.A. Lampert and P. Mark, Current Injection in Solids, Academic Press, New York, 1970.
- [62] R.D. Gould and C.J. Bowler, Thin Solid Films, 164 (1988) 281.
- [63] A.K. Hassan and R.D. Gould, Int. J. Electron., 69 (1990) 11.
- [64] J. Le Moigne and R. Even, J. Chem. Phys., 83 (1985) 6472.
- [65] N.F. Mott, Metal-Insulator Transitions, Taylor and Francis, London, 1974.
- [66] N.F. Mott and E.A. Davis, Electronic Processes in Non-crystalline Materials (2nd edn.), Oxford University Press, Oxford, 1979.
- [67] J.G. Simmons, Phys. Rev., 166 (1968) 912.
- [68] S.M. Sze, Physics of Semiconductor Devices (2nd edn.), Wiley, New York, 1981.
- [69] E.A. Rhoderick, Metal Semiconductor Contacts, Clarendon Press, Oxford, 1978.
- [70] G.M. Delacote, J.P. Fillard and F.J. Marco, Solid State Commun., 2 (1964) 373.
- [71] R.D. Gould, Thin Solid Films, 125 (1985) 63.
- [72] A.K. Hassan and R.D. Gould, J. Phys. D, 22 (1989) 1162.
- [73] A.K. Hassan and R.D. Gould, J. Phys. Condens. Matter, 1 (1989) 6679.
- [74] R.D. Gould and A.K. Hassan, Thin Solid Films, 193/194 (1990) 895.
- [75] T.S. Shafai and R.D. Gould, Int. J. Electron., 69 (1990) 3.
- [76] T.S. Shafai and R.D. Gould, Int. J. Electron., 73 (1992) 1043.
- [77] R.D. Gould and R.I.R. Blyth, Phys. Status Solidi A, 120 (1990) K57.

- [78] A.K. Hassan and R.D. Gould, *Int. J. Electron.*, **73** (1992) 1047.
- [79] A.K. Hassan and R.D. Gould, *Int. J. Electron.*, **74** (1993) 59.
- [80] S. Gravano, A.K. Hassan and R.D. Gould, *Int. J. Electron.*, **70** (1991) 477.
- [81] W. Wachawek and M. Ząbkowska-Wachawek, *Thin Solid Films*, **146** (1987) 1.
- [82] A. Twarowski, *J. Chem. Phys.*, **77** (1982) 5840.
- [83] A. Twarowski, *J. Chem. Phys.*, **77** (1982) 4693.
- [84] W. Mycielski, B. Ziólkowska and A. Lipiński, *Thin Solid Films*, **91** (1982) 335.
- [85] H. Laurs and G. Heiland, *Thin Solid Films*, **149** (1987) 129.
- [86] A.K. Jonscher and A.A. Ansari, *Philos. Mag.*, **23** (1971) 205.
- [87] A. Ahmad and R.A. Collins, *Phys. Status Solidi A*, **126** (1991) 411.
- [88] J. Kašpar, I. Emmer and R.A. Collins, *Int. J. Electron.*, **76** (1994) 793.
- [89] S.A. James, A.K. Ray and J. Silver, *Phys. Status Solidi A*, **129** (1992) 435.
- [90] R.D. Gould and A.K. Hassan, *Thin Solid Films*, **223** (1993) 334.
- [91] A.M. Saleh, R.D. Gould and A.K. Hassan, *Phys. Status Solidi A*, **139** (1993) 379.
- [92] S.I. Shihub and R.D. Gould, *Thin Solid Films*, **254** (1995) 187.
- [93] K.L. Chopra, *Thin Film Phenomena*, Kreiger, New York, 1979 (first published by McGraw Hill, New York, 1969).
- [94] D.V. Geppert, *J. Appl. Phys.*, **33** (1962) 2993.
- [95] M. Füstöss-Wégner, *Thin Solid Films*, **36** (1976) 89.
- [96] B.Sh. Barkhalov and Yu.A. Vidadi, *Thin Solid Films*, **40** (1977) L5.
- [97] F.-R. Fan and L.R. Faulkner, *J. Chem. Phys.*, **69** (1978) 3334.
- [98] A. Tripathi, A.K. Tripathi and A.R. Srivastava, *J. Electrostat.*, **16** (1984) 99.
- [99] Yu.A. Vidadi, K.Sh. Kocharli, B.Sh. Barkhalov and S.A. Sadreddinov, *Phys. Status Solidi A*, **33** (1976) K67.
- [100] K.J. Hall, J.S. Bonham and L.E. Lyons, *Aust. J. Chem.*, **31** (1978) 1661.
- [101] R.O. Loutfy, J.H. Sharp, C.K. Hsiao and R. Ho, *J. Appl. Phys.*, **52** (1981) 5218.
- [102] M. Martin, J.-J. André and J. Simon, *J. Appl. Phys.*, **54** (1983) 2792.
- [103] C. Hamann, A.V. Kovalchuk and M.V. Kurik, *Mater. Sci.*, **10** (1984) 109.
- [104] T.G. Abdel-Malik, A.A. Ahmed and A.S. Riad, *Phys. Status Solidi A*, **121** (1990) 507.
- [105] M. Shimura and N. Toyoda, *Jpn. J. Appl. Phys.*, **23** (1984) 1462.
- [106] S.K. Cheung and N.W. Cheung, *Appl. Phys. Lett.*, **49** (1986) 85.
- [107] R.S. Bradley, J.D. Grace and D.C. Munro, *J. Phys. Chem. Solids*, **25** (1964) 725.
- [108] J.J. Fendley and A.K. Jonscher, *J. Chem. Soc. Faraday Trans. I*, **69** (1973) 1213.
- [109] Y. Sadaoka and Y. Sakai, *J. Chem. Soc. Faraday Trans. II*, **72** (1976) 379.
- [110] W. Wachawek, M. Kulesza and M. Ząbkowska, *Mater. Sci.*, **7** (1981) 385.
- [111] H.S. Nalwa and P. Vasudevan, *J. Mater. Sci. Lett.*, **2** (1983) 22.
- [112] H.S. Nalwa and P. Vasudevan, *J. Mater. Sci. Lett.*, **4** (1985) 943.
- [113] T.G. Abdel-Malik, R.M. Abdel-Atif, M. El-Shabasy and M. Abdel-Hamid, *Indian J. Phys.*, **62A** (1988) 17.
- [114] Yu.A. Vidadi, L.D. Rozenshtein and E.A. Chistyakov, *Sov. Phys. Solid State*, **11** (1969) 173.
- [115] Yu.A. Vidadi, K.Sh. Kocharli, B.Sh. Barkhalov and S.A. Sadreddinov, *Phys. Status Solidi A*, **34** (1976) K77.
- [116] J.G. Simmons, G.S. Nadkarni and M.C. Lancaster, *J. Appl. Phys.*, **41** (1970) 538.
- [117] A.J. Twarowski and A.C. Albrecht, *J. Chem. Phys.*, **72** (1980) 1797.
- [118] M. Maitrot, G. Guillard, B. Boudjema, J.-J. André and J. Simon, *J. Appl. Phys.*, **60** (1986) 2396.
- [119] T.G. Abdel-Malik, *Thin Solid Films*, **205** (1991) 241.
- [120] S.R. Elliott, *Philos. Mag.*, **36** (1977) 1291.
- [121] S.R. Elliott, *Adv. Phys.*, **36** (1987) 135.
- [122] H. Büttger and V.V. Bryksin, *Hopping Conduction in Solids*, VCH, Deerfield Beach, FL, 1985.
- [123] A. Goswami and A.P. Goswami, *Thin Solid Films*, **16** (1973) 175.